Smart Structures and Systems, *Vol. 32, No. 1 (2023) 61-81*
https://doi.org/10.12989/sss.2023.32.1.061

An ensemble learning based Bayesian model updating approach for structural damage identification

Guangwei Lin [1,2,3a], Yi Zhang*[1,2,3], Enjian Cai [1,2,3b], Taisen Zhao [1,2,3c] and Zhaoyan Li [1,2d]

[1] *Key Laboratory of Earthquake Engineering and Engineering Vibration, Institute of Engineering Mechanics, China Earthquake Administration, China*
[2] *Key Laboratory of Earthquake Disaster Mitigation, Ministry of Emergency Management, China*
[3] *Department of Civil Engineering, Tsinghua University, Beijing, China*

(*Received December 24, 2022, Revised June 23, 2023, Accepted July 24, 2023*)

Abstract. This study presents an ensemble learning based Bayesian model updating approach for structural damage diagnosis. In the developed framework, the structure is initially decomposed into a set of substructures. The autoregressive moving average (ARMAX) model is established first for structural damage localization based structural motion equation. The wavelet packet decomposition is utilized to extract the damage-sensitive node energy in different frequency bands for constructing structural surrogate models. Four methods, including Kriging predictor (KRG), radial basis function neural network (RBFNN), support vector regression (SVR), and multivariate adaptive regression splines (MARS), are selected as candidate structural surrogate models. These models are then resampled by bootstrapping and combined to obtain an ensemble model by probabilistic ensemble. Meanwhile, the maximum entropy principal is adopted to search for new design points for sample space updating, yielding a more robust ensemble model. Through the iterations, a framework of surrogate ensemble learning based model updating with high model construction efficiency and accuracy is proposed. The specificities of the method are discussed and investigated in a case study.

Keywords: active learning; ensemble of surrogate; model updating; probabilistic ensemble; TMCMC

1. Introduction

Civil engineering structures and infrastructures are essential and intricate structural systems with a significant impact on economic, business, economic, and social aspects of life (Flah *et al*. 2021, He *et al*. 2018). Throughout their lifetime, these structures are exposed to a variety of excitations, including earthquakes, strong winds, traffic, operating activities, and excitations caused by humans (Güemes *et al*. 2020). Material deterioration is an additional significant challenge endangering structural safety and viability. In such situations, civil structures may sustain substantial damage, leading to catastrophic failure or even collapse (Sarmadi *et al*. 2021, Zhang *et al*. 2018). Structural health monitoring (SHM) is crucial for ensuring the safety of the structural systems and minimizing the financial and human life losses brought on by damage (Barazanchy *et al*. 2014, Ding *et al*. 2018, Mao *et al*. 2019). As an emergent tool for damage detection and structural condition assessment, SHM provides a way to infer the state of structural integrity and estimate the remaining useful life of a structural or mechanical system using measured data from sensors deployed on the systems (Cai and Zhang 2022, Erazo and Hernandez 2016, Nagarajaiah and Erazo 2016). One of the mainstream methods used in SHM is model updating, which can identify and update modal parameters via processing vibration signals (Abbasnia *et al*. 2018, Hoa *et al*. 2020).

Model updating techniques can be generally classified into matrix updating methods and parameter updating methods. The matrix updating methods are usually referring to the updating of stiffness or mass matrices (Panda and Modak 2022). However, matrix updating methods may violate structural connectivity so the updated parameters can hardly be related to the changes in the parameters of the model (Hou and Xia 2020). On the other hand, the updated objects of parameter updating methods are physical parameters. In the parameter updating approach, model parameters are updated to minimize an objective function which is the misfit between model-predicted data and measured data (Ren and Chen 2010, Sotoudehnia *et al*. 2019). In this sense, the parameter updating method is essentially an optimization problem. In this way, model updating methods reduce the uncertainty and make the model-predicted structural response close to reality.

Among all kinds of model updating approaches, Bayesian model updating has become one of the most popular techniques applied in various fields due to the benefit of managing uncertainties while taking into account prior knowledge (Alabi *et al*. 2018, Lin *et al*. 2021, Tran-

*Corresponding author, Associate Professor,
E-mail: zhang-yi@tsinghua.edu.cn
[a] Ph.D. Student, E-mail: lin-gw19@mails. tsinghua.edu.cn
[b] Ph.D. Student, E-mail: caienjian@qq.com
[c] Ph.D. Student, E-mail: az1321365458@qq.com
[d] Researcher, E-mail: lzhyiem@126.com

ISSN: 1738-1584 (Print), 1738-1991 (Online)

Ngoc *et al*. 2018). Bayesian model updating approach provides a coherent and rigorous probabilistic framework for characterizing and quantifying the uncertainties from material properties and the modeling errors for a robust structural prediction (Beck and Katafygiotis 1998, Cheung and Beck 2009, Zhang *et al*. 2020). In the framework of Bayesian model updating, the identification of structural model parameters is viewed from the perspective of probability statistics as a problem of solving the optimal model under the quantitative influence of model errors and measurement noises (Alkayem *et al*. 2018). Afterwards the structural model is updated to better describe the structural properties and facilitate effective decisions by taking into account dynamic response measurements (Hu and Yang 2018, Zhang *et al*. 2019). In the pioneering works, Collins *et al*. (1974) first proposed the Bayesian model parameter identification method. Beck and Katafygiotis (1998) built a more comprehensive and rigorous framework for Bayesian model updating and defined the concept of system identifications. Recently, numerous studies of Bayesian model updating have been developed on analyzing both numerical examples and real-world applications (Jiang *et al*. 2018, Lo and Leung 2019).

In contrast to conventional model updating methods, Bayesian model updating can identify a collection of structural models and obtain the modified model by averaging the models (Sousa *et al*. 2019). As a result, the Bayesian model updating technique is reliable and robust, and it is appropriate for outlining the uncertainties associated with modeling structural systems (Kwag and Gupta 2018, Wang and Shafieezadeh 2020). In the Bayesian updating framework, the posterior distribution of updating physical parameters is expressed as a product of the prior distribution and the likelihood function. However, with the increase in parameter dimensions, the model updating problem may become unidentifiable. The analytical form of the posterior probability density function (PDF) may not be available. Even with linear models, the model updating problem may be potentially ill-posed, i.e., the problem is not globally identifiable. The problem becomes even more challenging when only some of the degrees of freedom (DOF) of the model are measured. To perform an efficient Bayesian model updating analysis, a robust sampling algorithm like Markov chain Monte Carlo (MCMC) is required (Martino 2018). In this study, transitional Markov Chain Monte Carlo (TMCMC) is employed algorithm due to its excellent performance in high-dimensional model updating problems and complex distributions (Ching and Chen 2007).

Furthermore, there are still some difficulties with Bayesian model updating in complicated systems. One of the main limitations of model updating methodologies in engineering applications is computational efficiency, which is particularly pronounced in complex and high-dimensional scenarios (Kirschner *et al*. 2019). Two solutions to this issue are dimension reduction technology based on substructure division and the creation of surrogate models.

In the substructuring methods, a global structure is divided up into a number of distinct substructures. Re-analysis of the global structure can be prevented by just analyzing the substructures (Wang *et al*. 2021, Weng *et al*. 2020). Each substructure retains smaller number degrees of freedom (DOFs) compared with the whole structure. Through this division technique, it is suitable for reducing the dimension of complex high-dimensional problems and enhancing computational efficiency (Beniddir *et al*. 2021, DeVore *et al*. 2016). Up to now, many scholars have studied the application of substructure division in civil structures and systems (Huang *et al*. 2021, Li and Hao 2014, Zhu *et al*. 2021). Different from the direct identification by substructure division in previous studies, the parameter identification and damage diagnosis in this study are divided into two steps. First, the substructure division and ARMAX time series analysis technology (Azim *et al*. 2020; Mei *et al*. 2019) are used to locate the damaged substructure, and then the located damaged substructure is further investigated and analyzed for the subsequent quantitative damage analysis.

An alternative strategy for high-dimensional complex structures is to simplify the problem with a surrogate model. Besides, the explicit expression of the likelihood function may be difficult or even impossible since the models are often in numerical form rather than functional form, making it challenging to establish a connection between physical parameters and structural measured output variables (also termed as “features” in the following context). This has additionally emerged as a driving factor for the application of surrogate models in Bayesian model updating. Surrogate models can be used to approximate the structural responses at predetermined sampling points dispersed across the design space at a significantly lesser cost (Alexander *et al*. 2008, Bisbo and Hammer 2020, Jiang *et al*. 2020). Many academics have utilized surrogate models in civil engineering including the polynomial response surface model (Khatir *et al*. 2019), radial basis function (Elias *et al*. 2020, Li *et al*. 2018, Park *et al*. 2019), Kriging model (Mao *et al*. 2020, Qin *et al*. 2018), support vector regression (SVR) (Alkayem *et al*. 2018, Wang and Cha 2021).

Before building the surrogate models, feature extraction has to be conducted to further identify the hidden information of structural conditions from the structural features. However, if the measured acceleration or displacement is directly taken as the structural feature, it may lead to ill-conditioned problems. (Ching and Beck 2003). In many research, the measured time history data are employed for modal identification, and subsequently modal parameters like frequency are used for damage detection (Krishansamy and Arumulla 2018, Zhu *et al*. 2020). However, modal parameters like frequency are not sensitive enough to damage, especially local damage (Mei *et al*. 2019). Wavelet packet decomposition (WPD) is a multi-resolution time-domain analysis method with high damage sensitivity, including local damage. Compared with wavelet decomposition, WPD can decompose the high-frequency part of the signal in more detail (Effendi *et al*. 2019, Liao *et al*. 2021, Liu *et al*. 2021). This advantage makes WPD widely used to identify structural damage. Therefore, this paper employs the l_p norm of the node energy of the signal after WPD as the structural feature, leading to a better mapping between physical parameters and structural

vibration information.

However, a single surrogate model has been proven to be computationally prohibitive for tackling high-dimensional problems due to the curse of dimensionality, despite being successful in a range of technical applications (Li *et al*. 2021, Ye *et al*. 2018). Furthermore, different surrogate models are appropriate for various problems (Alizadeh *et al*. 2019). A single surrogate model is quite efficient for some particular situations, while for other situations would be quite inefficient (Xing *et al*. 2019). The ensemble of surrogates (EOS), a weighted average surrogate model, has proven to be a statistically more accurate and resilient solution (Goel *et al*. 2007), which could improve the accuracy of model updating. The fundamental idea behind EOS is that multiple models are trained as ensemble members and their outputs are combined into a single output in order to provide reasonable and appropriate performance. Rather than emphasizing the creation of unique and diverse surrogate models, this method stresses the combination or selection of the foundation surrogate models. (Dhamotharan *et al*. 2018).

Nevertheless, during the last decade, ensemble research efforts in the engineering field have primarily focused on the linear weighted averages of surrogate predictions based on performance measures (or error measures) of both local and global natures (Queipo and Nava 2019). There are two issues with this strategy. First, the weighted average of each model will be superior to the worst model but inferior to the best model, which will not change because of the accuracy and effectiveness of the performance measurement. If the posterior probabilities of the outputs of multiple surrogate models at the same design point are higher than those at other design points, it is anticipated that EOS will raise overall confidence rather than reduce it. Besides, such linear weighted average of surrogate models also fails to incorporate cues from the weak model. It is noteworthy that a new study (Chen *et al*. 2022) develops a probabilistic ensembling approach for object detection with multimodal signals, which is derived from Bayesian inference. Although academics focus on multimodal object detection, it seems quite beneficial for EOS. Therefore, the probabilistic ensemble method is introduced in this study and combined with bootstrapping as the first part of the proposed EOS framework. Before describing the second part of the framework, it is necessary to discuss another issue in the existing EOS research mentioned above that they frequently concentrate on constructing error metrics rather than updating the sample space. The update of the sample space is also called active learning, which allows users to search for a more reasonable and accurate sample space. The current research on active learning focuses on the expected improvement (EI) criterion (Berk *et al*. 2018, Sener and Savarese 2017, Siddiqui *et al*. 2020). The purpose of EI criterion is to search for design points that can update the maximum (or minimum) of surrogate models as new sample points. Unfortunately, its premise is that the optimization direction of the surrogate model is to seek the extreme value, which is similar to the cost function. In this study, however, the optimization objective of the surrogate models is to reduce the difference between the calculated structural response and the measured response. In the sample space updating phase, we should first select the points to be added, and then use the finite element model to calculate the corresponding response value as the training data of the model. Therefore, we cannot know in advance which points will make a small difference between the predicted response value of the surrogate model and the measured response. Thus, EI criterion is unavailable in this study. Some other research develops the infill criterion based on Kriging model, which is to select points with large prediction variance to be added into sample space. However, this approach solely regards the prediction error as a random variable subject to the Gaussian distribution, and does not treat the input parameters in the surrogate models as random variables. To overcome this shortcoming, this study uses Monte Carlo sampling to obtain the PDF of the output of each surrogate model and then apply the previously mentioned probability ensemble method to acquire their PDF after ensemble in the second part of the EOS framework. Next, new sample points are chosen to add to the sample space in accordance with the maximum entropy principle.

The innovation of this paper is reflected in the following two aspects: (1) this paper combines the probabilistic ensemble method with bootstrapping and maximum entropy principle, and proposes a novel EOS framework which is superior to the existing EOS methods and active learning approach in both accuracy and reasonability; (2) this paper develops a three-step Bayesian model updating process consisting of the ARMAX and substructure division based damage localization, the construction of surrogate models based on the sample space updating, and the surrogate ensemble learning based model updating. In the damage localization phase, the structural system is divided into several subsystems, each of which is represented by a surrogate model with relatively small input/output vectors, to avoid high-dimensional representations. Then ARMAX model is used to search for the damaged substructure. In the construction of surrogate models, the wavelet packet decomposition technology is first employed to extract damage-sensitive feature vectors as the output of the surrogate model, and then the developed EOS framework is able to update the sample space and construct a series of accurate and robust surrogate models. In the surrogate ensemble learning based model updating, the posterior PDF of individual surrogate models are fused by probability ensemble approach. The final ensemble posterior PDF serves as the foundation for subsequent parameter updating, damage identification, and uncertainty quantification.

The remainder of this paper is organized as follows. Section 2 presents the methodology, including the damage localization, the construction of surrogate models, and the framework of surrogate ensemble learning based model updating. Section 3 presents an example analysis to demonstrate the effectiveness of the proposed three-step Bayesian model updating process. Final research findings are given in Section 4.

2. Methodology

2.1 ARMAX based damage localization

The first step in the three-step Bayesian model updating process proposed in this paper is the ARMAX based damage location. ARMAX creates a generalized mathematical description of the nonlinear dynamical system with stochastic noise and integrates the variation of input parameters into the system model (Do *et al*. 2019). The main advantage of the ARMAX model is that it inherently mitigates signals with noise from various sources, providing unbiased parameter estimates.

Initially, healthy data is created from the acceleration signals obtained in the known healthy state of the structure. Similarly, several databases which consist of the acceleration data from the unknown condition are formed. By philosophy, these unknown signals are processed by comparing with the health data on the condition of the structure using a suitable ARMAX model. The normalized root mean square (NRMSE) is used to measure the goodness of the fit between the simulated response $\hat{x}$ and measurement data x.

$$NRMSE = \frac{(x-\hat{x})^T(x-\hat{x})}{x^T x} \tag{1}$$

Before calculating the NRMSE, the acceleration signals need to be decorrelated to increase the robustness of the technique. In the process of decorrelation, the m-dimension time series signals $x(t)$ are pre-processed by following

$$S(t) = Mx(t) \tag{2}$$

where $S(t)$ represents the de-correlated signals, and M is the $m \times m$ matrix, chosen to ensure the covariance matrix R_{yy} to be the unit matrix I as

$$\begin{aligned} R_{yy} &= E(S(t)S(t)^T) = E(Mx(t)x(t)^T M^T) \\ &= MR_{xx}M^T = I \end{aligned} \tag{3}$$

The covariance matrix R_{xx} is usually symmetric and positive definite, hence it is decomposed as follows

$$R_{xx} = \psi_x \omega_x^{1/2} \omega_x^{1/2} \psi_x^T \tag{4}$$

where ψ_x is an orthogonal matrix and ω_x = diag $\{\lambda_1, \lambda_2, ..., \lambda_m\}$ denotes a diagonal matrix with positive eigenvalues $\lambda_1 \geq \lambda_2 \geq ... \geq \lambda_m$. Therefore, the matrix M can be computed as

$$M = V\omega_x^{-1/2}\psi_x^T \tag{5}$$

where V is an arbitrary orthogonal matrix. Thus, the components of the de-correlated signals $S(t)$ are mutually uncorrelated and they have unit variance. The ARMAX model is given by the difference equation (Candy 2005)

$$A(q)S(t) = B(q)u(t) + C(q)e(t) \tag{6}$$

where A, B, and C are transfer operators dimensioned with integers N_a, N_b, and N_c, respectively; S is system output; u is system input; $e(t)$ is noise sequences (assumed to be white noise); q^{-1} is the backward shift operator (also termed as time delay), that is

$$u(t-1) = u(t)q^{-1} \tag{7}$$

The transfer operators A, B, and C can be further expanded as

$$\begin{cases} A(q) = 1 + a_1 q^{-1} + \cdots + a_{n_a} q^{-n_a} \\ B(q) = b_1 + \cdots + b_{n_b} q^{-(n_b-1)} \\ C(q) = 1 + c_1 q^{-1} + \cdots + c_{n_c} q^{-n_c} \end{cases} \tag{8}$$

2.2 Surrogate model

2.2.1 Feature extraction based on wavelet packet decomposition

Suppose $S(t)$ is the original acceleration signal measured by the sensor, it can be expressed as

$$S(t) = \sum_{j=1}^{2^k} S_{kj}(t) \tag{9}$$

where k is the decomposition level, and $S_{kj}(t)$ is the quadrature band sub-signal, expressed as

$$S_{kj}(t) = \sum c_{kj}^i \, \phi_{j,k,i}(t) \tag{10}$$

where $\phi_{j,k,i}(t)$ is a wavelet packet. The energy at position j of the kth layer obtained by wavelet packet decomposition can be expressed as

$$E_{kj} = \int \left| S_{kj}(t) \right|^2 dt \tag{11}$$

The feature vector y is chosen as the lp norm of the last layer of the wavelet packet decomposition

$$y = l^p = \sum_{j=1}^{2^k} \left| E_{kj} \right|^p, \quad 1 < p < 2 \tag{12}$$

In this section, four commonly used surrogate models, namely, Kriging, RBF neural networks (RBFNN), SVR, and Multivariate Adaptive Regression Splines (MARS) are briefly reviewed, and then adopted to construct an ensemble of surrogates. Kriging is particularly well-suited to model local variations, attaining both local and global modeling capabilities (Abbasnia *et al*. 2018). The selection of SVR is based on its capability to effectively capture complex relationships between input and output variables, particularly when dealing with limited sample data (Christelis *et al*. 2019). RBFNN performs well in small and rare samples (Fei and Wang 2019). MARS is recognized for its rapid, flexible, adaptive, and nonparametric approach to

regression model development (Roy and Datta 2019).

2.2.2 Kriging

The Kriging model, sometimes referred to as the Gaussian process, tends to identify the best unbiased linear predictor while minimizing the mean square error of the prediction (Krige 1951). Because of its excellent fitting capabilities, Kriging is frequently employed in engineering (Houret *et al*. 2019). The universal Kriging model could be expressed as the summation of a polynomial term used to predict global trends and a stationary Gaussian random process term used for local deviation regression

$$f_1(x) = F(\beta, x) + z(x) = \sum_{j=1}^{k} \beta_j f_j(x) + z(x) \tag{13}$$

where x denotes the training sample, $F(\beta,x)$ represents the regression model composed of the regression parameters β_j and the polynomial functions $F(\beta,x)$; and $z(x)$ is a standard Gaussian random process representing the noise, whose covariance function can be written as a kernel function

$$Cov[z(x_i), z(x_j)] = \sigma^2 R(\theta, x_i, x_j) \tag{14}$$

where σ^2 is the process variance; x_i and x_j are the components of x; R stands for the admissible correlation coefficient with hyper-parameter, which regulates the smoothness and the predictive accuracy of the Kriging model (Cheng and Lu 2020). The unknown parameters $(\beta,\sigma^2,\theta)$of the Kriging model can be optimized by maximum likelihood estimation. Once the optimal values of the three parameters are obtained, the expected value $\mu_{\hat{y}}^2$ and the variance $\sigma_{\hat{y}}^2$ at a point x can be determined by the following equations

$$\mu_{\hat{y}}(x) = f^T(x)\beta + r^T(x)R^{-1}(Y - F\beta) \tag{15}$$

$$\begin{aligned}\sigma_{\hat{y}}^2 = \sigma^2(1 - r^T(x)R^{-1}r(x) \\ +(f(x) - FR^{-1}r(x))^T(FR^{-1}F)^{-1}(f(x) \\ -FR^{-1}r(x)))\end{aligned} \tag{16}$$

where $f(x) = \{f_1(x),\ldots, f_k(x)\}^T$ is the basis function; $F = \{f(x_1),\ldots, f_k(x_n)\}^T$; $r(x) = \{R(x,x_1),\ldots, R(x,x_n)\}^T$ represents the correlation vector between the unknown point x and n observed points.

2.2.3 RBF neural networks

RBFNN is a specific variety of the multilayer neural network that has matured as one of the most widely used classifiers in the literature. The RBFNN has a high learning efficiency and a decent tolerance for the noise in the dataset. RBFNN represents a three-layered architecture, taking inputs from the dataset as its first layer. The output layer, which creates the prediction, is in the third layer. A non-linear RBF activation function is present in the middle layer, which is referred to as the hidden layer. The RBFNNs are a subclass of functions whose response monotonically grows or decays with respect to the distance from a central point. The RBFNN begins by determining the Euclidean distance from the evaluated point to each neuron's center. Then, by applying an RBF to the distance, the influence of each neuron is measured. The most widely used RBF in the literature is the Gaussian function, which is defined as follows

$$\phi_j(\theta) = exp\left(-\frac{(x - c_j)^2}{2\sigma_j^2}\right) \tag{17}$$

where ϕ_i is the RBF of the jth RBF neuron, $x = (x_1,x_2,\ldots, x_d)^T$ is the input vector, c_j is the center value of the Gaussian function, j represents the sample number, and σ_j^2 represents the variance of the Gaussian function. Thus, the output of RBFNN is calculated via linear superposition

$$f_2 = \sum_{j=1}^{p} w_j \phi_j \tag{18}$$

where y is the output of the RBFNN, p is the number of RBF neurons, and w_j is the weight assigned from the jth RBF neuron to the output layer (Qasem and Shamsuddin 2011).

2.2.4 Support vector regression

SVR can create a regression function between the input and output of the original model to replace the original model (Ren *et al*. 2020). The expression of the mapping relationship between model input x and output y is formulated as (Vapnik 1999)

$$y(x) = \omega^T \phi(x) + b \tag{19}$$

where $\phi(x)$ denotes the mapping function, ω is the coefficient vector and b is a constant. SVR aims to make the deviation between the predictive feature and the real target less than ε. As a result, the optimal regression function may be transformed into an optimization problem, and the values of ω and b can be determined by using the following equations

$$\begin{aligned} &min\ \ \frac{1}{2}\|\omega\|^2 + C\frac{1}{l}\sum_{i=1}^{l}(\xi_i + \xi_i^*) \\ &s.t.\begin{cases} y_i - \omega^T\phi(x_i) - b \le \varepsilon + \xi_i \\ \omega^T\phi(x_i) + b - y_i \le \varepsilon + \xi_i^* \\ \xi_i, \xi_i^* \ge 0, \quad i = 1,2\ldots, l \end{cases} \end{aligned} \tag{20}$$

where ξ_i and ξ_i^* represent slack variables, l is the total number of samples, ε stands for the training error, and C denotes the penalty factor. By introducing the Lagrangian function, Eq. (10) can be recast as following

$$\begin{aligned} &min\ \sum_{i=1}^{l} y_i(\alpha_i - \alpha_i^*) \\ &-\frac{1}{2}\sum_{i,j=1}^{l}(\alpha_i - \alpha_i^*)(\alpha_i - \alpha_i^*)K(x_i, x_j) \end{aligned} \tag{21}$$

$$s.t.\begin{cases}\sum_{i,j=1}^{l}(\alpha_i-\alpha_i^*)=0\\ \alpha_i,\alpha_i^*\in[0,C]\end{cases} \tag{21}$$

where $K = (x_i,x_j)$ represents the kernel function, expressed as follows

$$K(x_i,x_j)=\exp\left(-\gamma\left\|x_i-x_j\right\|^2\right),\ \gamma\geq 0 \tag{22}$$

where γ represents the nuclear parameters. The expression to calculate the predicted value is

$$f_3(x)=\sum_{i=1}^{l}(\alpha_i-\alpha_i^*)\,K(x_i,x_j)+b \tag{23}$$

2.2.5 MARS model

MARS is a nonlinear, nonparametric regression methodology, capable to examine the intricate nonlinear relationships between a response variable and predictor variables (Adnan *et al*. 2020). MARS was first introduced by Friedman (1991) as a flexible procedure to organize relationships between a group of input variables and the target dependent variables that are almost additive or involve interactions with fewer variables. It is a nonparametric statistical method based on a divide and conquer strategy in which the training data sets are partitioned into discrete piecewise linear segments, also referred to as splines, of various gradients. The real benefit of the MARS model over other black-box machine learning techniques, such as the ANN model, is that it thoroughly explores the relationship between output and input variables (Naser *et al*. 2022).

MARS makes no assumptions regarding the underlying functional relationships between dependent and independent variables. The splines are typically connected smoothly, and the piecewise curves, often referred to as the basis functions, produce a flexible model that can accommodate both linear and nonlinear behavior. The connection points between the pieces are called knots. MARS differs from other well-known parametric linear regression approaches in that it provides additional flexibility for studying the nonlinear interactions between an input and response variable. The approach may successfully trace hidden relationships in a high-dimensional dataset as well as the complex structures evident in data points since it considers all interactions and functional forms between input variables (Naser *et al*. 2022). The most general form of the MARS model $y(x)$, which is a linear combination of the basis functions and their interactions, is given below

$$f_4(x)=\beta_0+\sum_{m=1}^{M}\beta_m\,\lambda_m(x) \tag{24}$$

where $y(x)$ is the expected response, β_0 and β_m are coefficients that are generated using the least-squares method to provide the best data fit, and m is the number of basis functions in the model. The term λ_m is a basis function, following the form $\max(0,x-c)$ with a knot defined at value t.

$$max(0,x-t)=\begin{cases}x-t,\ if\ x\geq t\\ 0,\ otherwise\end{cases} \tag{25}$$

2.3 Framework of surrogate ensemble learning based model updating

The proposed framework of surrogate ensemble learning based model updating consists of sample space updating and EOS based model updating. First, assume that Θ is the design space and the initial sample set is $D_0(\theta,y)$, where $\theta = \{\theta_1,\ldots,\theta_N\}\in\Theta$ and $y = \{y_1,\ldots, y_N\}$. Use the bootstrapping method to obtain the j subsets $D_j^{(t)}$, $t = 0, 1,\ldots,q$, where q denotes the number of the sample space updating. For each subset $D_j^{(t)}$, Kriging, RBFNN, SVR, and MARS are employed to construct surrogate models $\hat{y}_{i,j}=f_{i,j}^{(t)}(\theta)$, where $i = 1$ for Kriging, $i = 2$ for RBFNN, $i =3$ for SVR, and $i = 4$ for MARS. By averaging the surrogate models of the same method under different subsets $D_j^{(t)}$ to obtain four surrogate models $f_i^{(t)}(\theta)=\sum_j f_{i,j}^{(t)}(\theta)$ for subsequent derivation. To acquire the PDF of the output of the surrogate model, Monte Carlo is utilized to draw the samples $\theta_{MC} = \{\theta_1,\ldots, \theta_m\}\in\Theta$. Then the corresponding surrogate model output is given as $f_i^{(t)}(\theta_{MC},D^{(t)})$. Divide Θ into p intervals $\{\Theta_1,\ldots, \Theta_m\}$, and the probability mass function (PMF) of the output of each surrogate model can be expressed as

$$p\left(\hat{y}|\theta;f_i^{(t)}\left(\theta,D^{(t)}\right)\right)=\frac{Count\ f_i^{(t)}\left(\theta_{MC},D^{(t)}\right)}{m}\quad \theta\in\Theta^k\ \ 1\leq k\leq p \tag{26}$$

Next, the PMFs are replaced with PDFs for subsequent derivation. Crucially, the output of each surrogate model is assumed to be conditionally independent given the updated physical parameter θ

$$\begin{aligned}&p(\hat{y}|\theta;f_1^{(t)}(\theta,D^{(t)}),\ldots,f_n^{(t)}(\theta,D^{(t)}))\\&=\prod_{i=1}^{n}p(\hat{y}|\theta;f_i^{(t)}(\theta,D^{(t)}))\end{aligned} \tag{27}$$

On the basis of Bayesian inference, the updated parameters θ can be inferred by the posterior PDF given the prior PDF $p(\theta)$

$$\begin{aligned}&p(\theta|\hat{y};f_1^{(t)}(\theta,D^{(t)}),\ldots,f_n^{(t)}(\theta,D^{(t)}))\\&=\frac{p(\hat{y}|\theta;f_1^{(t)}(\theta,D^{(t)}),\ldots,f_n^{(t)}(\theta,D^{(t)}))p(\theta)}{p(\hat{y}|f_1^{(t)}(\theta,D^{(t)}),\ldots,f_n^{(t)}(\theta,D^{(t)}))}\\&=\frac{1}{Z}\prod_{i=1}^{n}p(\hat{y}|\theta;f_i^{(t)}(\theta,D^{(t)}))\,p(\theta)\end{aligned} \tag{28}$$

where $Z=p(\hat{y}|f_1^{(t)}(\theta,D^{(t)}),\ldots,f_n^{(t)}(\theta,D^{(t)}))$ is normalized

constant (or evidence). $p(\hat{y}|\theta; f_1^{(t)}(\theta, D^{(t)}), \ldots, f_n^{(t)}(\theta, D^{(t)}))$ in Eq. (28) is the likelihood function, while that in Eqs. (26)-(27) is the conditional probability. Although the meanings are different, they have the same mathematical expression, which can be regarded as the same thing in the derivation. The uncertainty of a single sample point can be quantified by the information entropy

$$H(\theta) = -\frac{1}{Z}\prod_{i=1}^{n} p(\hat{y}|\theta; f_i^{(t)}(\theta, D^{(t)}))\, p(\theta) \left[\sum_{i=1}^{n} ln\, p\left(\hat{y}|\theta; f_i^{(t)}\left(\theta, D^{(t)}\right)\right) + ln\, p\,(\theta) - ln\, Z\right] \tag{29}$$

Then l candidate points $\theta_{add} = \{\theta_1,\ldots,\theta_l\} \in \Theta$ are sampled for updating $D^{(t)}$, and the points $\theta^{(t+1)}$ with the largest information entropy are selected as the updating points. The corresponding structural feature $y^{(t+1)}$ are calculated by the finite element model.

$$\begin{cases} \theta^{(t+1)} = \underset{\theta_{add}}{argmax} H(\theta) \\ D^{(t+1)} = D^{(t)} \bigcup \{\theta^{(t+1)}, y^{(t+1)}\} \end{cases} \tag{30}$$

Then $D^{(t+1)}$ is used to build the new surrogate models $\hat{y}_i = f_i^{(t+1)}(\theta)$. Stop such iteration until the total number of sample points $N + q$ meets the requirements. The sample space updating steps are summarized in Algorithm 1.

Algorithm 1 Sample space updating

1. Input: prior PDF $p(\theta)$; design space Θ; Initial sample set $D_0 = (\theta, y)$, where $\theta = \{\theta_1,\ldots,\theta_N\} \in \Theta$ and $y = \{y_1,\ldots, y_N\}$
2. Select j number of random subsets $D_j^{(t)}$ from $D^{(t)}$ by bootstrapping method for $t = 0, 1,\ldots,q$
3. Construct i surrogate models $\hat{y}_{i,j} = f_{i,j}^{(t)}(\theta)$ for each subset, and obtain the average model
4. Draw the samples $\theta_{MC}=\{\theta_1,\ldots, \theta_m\} \in \Theta$ and calculate $p(\hat{y}|f_1^{(t)}(\theta, D^{(t)}), \ldots, f_n^{(t)}(\theta, D^{(t)}))$ by Eq. (25) and (26)
5. Sample l candidate points $\theta_{add} = \{\theta_1,\ldots,\theta_l\} \in \Theta$ and calculate corresponding entropy by Eq. (28)
6. Calculate $D^{(t+1)}$ by Eq. (29)
7. If $N+q$ meets the requirements, end; otherwise go to step 2

After obtaining the final surrogate models $\hat{y}_i = f_i^{(q)}(\theta)$. Uncertain parameters can be inferred based on the posterior PDFs

$$p(\theta|y; f_1^{(q)}(\theta, D^{(q)}), \ldots, f_n^{(q)}(\theta, D^{(q)})) \propto \prod_{i=1}^{n} p(y|\theta; f_i^{(q)}(\theta, D^{(q)}))\, p(\theta) \tag{31}$$

where $p(y|\theta; f_1^{(t)}(\theta, D^{(t)}), \ldots, f_n^{(t)}(\theta, D^{(t)}))$ is the likelihood function, and y is the measured features. Noted that the likelihood function here is different from that in Eq. (28) for the modeling and measurement noise ε. The relationship between y and $\hat{y}$ can be expressed as

$$y_i = \hat{y}_i + \varepsilon_i = f_i^{(q)}(\theta, D^{(q)}) + \varepsilon_i \tag{32}$$

where ε_i is often taken as a Gaussian random variable with zero mean and variance σ_ε^2

$$p(\varepsilon_i) = \frac{1}{\sqrt{2\pi}\sigma_\varepsilon} exp\left(-\frac{\varepsilon_i^2}{2\sigma_\varepsilon^2}\right) \tag{33}$$

By substituting Eq. (32) into Eq. (33), the likelihood function can be obtained by the statistically independent assumption of ε_i

$$p(y|\theta; f_i^{(q)}(\theta, D^{(q)})) = \frac{1}{\sqrt{2\pi}\sigma_\varepsilon} exp\left(-\frac{y - f_i^{(q)}\left(\theta, D^{(q)}\right)^2}{2\sigma_\varepsilon^2}\right) \tag{34}$$

For an individual surrogate model, Eq. (31) can be simplified to

$$p(\theta|y; f_i^{(q)}(\theta, D^{(q)})) = \frac{p(y|\theta; f_i^{(q)}(\theta, D^{(q)}))p(\theta)}{p(y|f_i^{(q)}(\theta, D^{(q)})))} \propto p(y|\theta; f_i^{(q)}(\theta, D^{(q)}))p(\theta) \tag{35}$$

By applying the conditional independence assumption from Eq. (35) to Eq. (31), we can give an approach for EOS as

$$p(\theta|y; f_1^{(q)}(\theta, D^{(q)}), \ldots, f_n^{(q)}(\theta, D^{(q)})) \propto \prod_{i=1}^{n} p(y|\theta; f_i^{(q)}(\theta, D^{(q)}))\, p(\theta) \propto \frac{\prod_{i=1}^{n} p(\theta|y; f_i^{(q)}(\theta, D^{(q)}))}{p(\theta)^{n-1}} \tag{36}$$

However, in the general case, the direct integral of the posterior distribution is laborious and impractical. The posterior distribution can be approximated effectively through sampling. Because of its great accuracy and straightforward underlying theory, Monte Carlo simulation (MCS) is recognized as an appropriate tool for stochastic analysis. However, the extensive calculation is a barrier to its application. Furthermore, it is frequently impossible to determine structural response and parameters since the density of the posterior PDF is concentrated in a very small subset of the parameter space. Therefore, the transitional Markov chain Monte Carlo (TMCMC) method is preferred. TMCMC converges to the posterior PDF via a series of intermediate PDFs (Ching and Chen 2007). It is quite helpful for drawing samples from complicated PDFs. Nevertheless, with TMCMC, kernel density estimation is

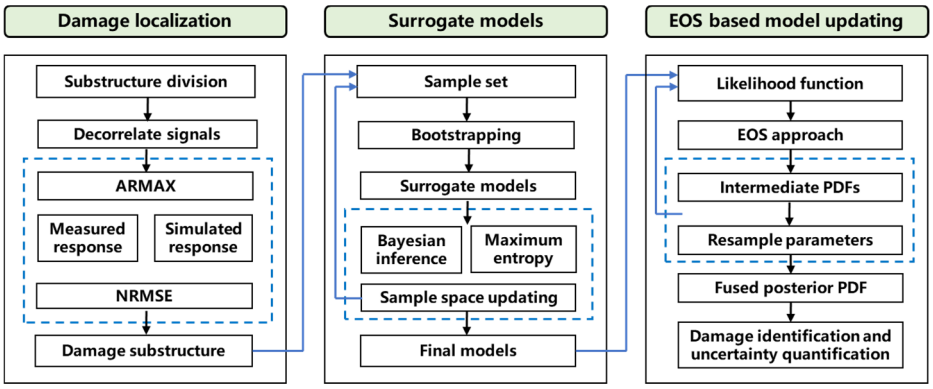

Fig. 1 Flow chart of the three-step Bayesian model updating framework

not required. In order to handle high-dimensional PDFs more effectively, a resampling approach is used. TMCMC also permits the calculation of evidence Z, which is essential for Bayesian model class selection. The sequence of intermediate PDFs in TMCMC is

$$p^{(j)}(\theta) \propto p(\theta^{(j-1)}) \prod_{i=1}^{n} p\left(y|\theta; f_i^{(q)}\left(\theta^{(j-1)}, D^{(q)}\right)\right)^{p_j} \quad (37)$$

where j denotes the iteration stage. $p_i^{(j)}$ starts from $p_0 = 0$ and progressively until p_n reaches one. $\theta^{(j-1)} = \left\{\theta_1^{(j-1)}, \ldots, \theta_{N_j}^{(j-1)}\right\}$ denotes samples drawn from $p_i^{(j-1)}$, and $\theta^{(0)}$ is the prior samples. Before adaptive computing p_{j+1}, the plausibility weights need to be calculated

$$\begin{aligned} & w\left(\theta_k^{(j-1)}\right) \\ &= \frac{p\left(\theta_k^{(j-1)}\right) \prod_{i=1}^{n} p\left(y|\theta; f_i^{(q)}\left(\theta^{(j-1)}, D^{(q)}\right)\right)^{p_j}}{p\left(\theta_k^{(j-1)}\right) \prod_{i=1}^{n} p\left(y|\theta; f_i^{(q)}\left(\theta^{(j-1)}, D^{(q)}\right)\right)^{p_{j-1}}} \\ &= p\left(\theta_k^{(j-1)}\right) \prod_{i=1}^{n} p\left(y|\theta; f_i^{(q)}\left(\theta^{(j-1)}, D^{(q)}\right)\right)^{p_j - p_{j-1}}, \\ & k = 1,2,\ldots,N_j \end{aligned} \quad (38)$$

where $w(\theta_{N_j}^{(j-1)})$ indicates the distance between $p_j(\theta)$ and $p_{j-1}(\theta)$, reflecting the iteration speed of the intermediate PDFs converging to the target distribution. A common assumption of the coefficient of variation (C.O.V) of this value is the unity which is adopted in this study (Ching and Chen 2007). The updating parameters are resampled by

$$\theta_k^{(j-1)} = \theta_l^{(j-1)} \text{with the probabillity } \frac{w(\theta_k^{(j-1)})}{\sum_{l=1}^{N_j} w(\theta_l^{(j-1)})}, \quad k = 1,2,\ldots,N_j \quad (39)$$

Algorithm 2 EOS based model updating

1. Input: final surrogate models $\hat{y}_i = f_i^{(q)}(\theta)$ in Algorithm 1; measured features y; prior PDF $p(\theta) = p^{(0)}(\theta)$
2. Construct likelihood function PDFs under each surrogate model with $\theta^{(j-1)}$ by Eq. (33)
3. Calculate intermediate PDF $p^{(j)}(\theta)$ by Eq. (36) and resample updating parameters $\theta^{(j)}$ by Eq. (38)
4. Do steps 2-3 until $p_j = 1$
5. Output: Fused posterior PDF $p^{(n)}(\theta)$

Based on the above-mentioned techniques, the three-step Bayesian model updating process in this paper is illustrated in Fig. 1. First, the substructure division and ARMAX are used for damage localization. Then surrogate models are built on the damaged substructure. Bootstrapping method and maximum entropy principle are utilized for sample space updating. Finally, the fused ensemble posterior PDFs are obtained by probability ensemble and TMCMC. The performance of the developed framework will be investigated in the following section.

3. Case study-four storey frame

3.1 Problem description

In this section, a numerical study is conducted to investigate the performance of the proposed EOS framework and the three-step Bayesian model updating process. For this purpose, a ten-storey frame structure subjected to seismic acceleration $\ddot{x}_g(t)$ are considered as shown in Fig. 3. The typical acceleration responses of the first storey in the undamaged state caused by the seismic excitations are shown in Fig. 3(a). Since measured responses always contain some level of corrupted noise, noise with 1% variance of the signal-to-noise ratio (NSR) was randomly added to the computed responses to simulate this situation as Fig. 3(b) demonstrates. The excitation time is 20 s and the acquisition frequency is 100 Hz. Therefore, the acceleration time history measured by a single sensor consists of 2000 data points. The frame has a dimension of 15 m × 10 m with a height of 31.5 meters. The first storey

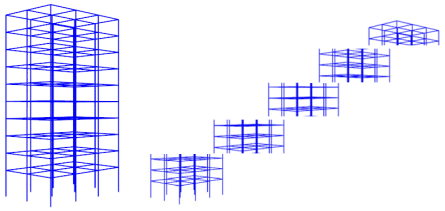

Fig. 2 The ten-storey frame

is 4.5 meters high, while the other storeys are 3 meters high. The damping of the structure adopts Rayleigh damping.

To reduce the complexity of the problem, the ten-storey frame is divided into five small substructures as Fig. 2 shows. The first four substructures consist of three storeys whereas the top substructure is composed of two storeys, and there are overlapping storeys among the substructures. In each substructure, a series of low-dimensional surrogate models are used to map the uncertain physical parameters to the structural responses. The updated parameters of the odd storey are averaged by the updated values of the corresponding surrogate models of the two adjacent substructures containing the storey. The unscaled inter-storey stiffness and mass density of each storey are used as the updated parameters, which can be expressed as

$$\begin{cases} \theta_{2i-1} = k_i/k_0 & \text{for } \ i = 1,2,\dots,10 \\ \theta_{2i} = m_i/m_0 & \text{for } \ i = 1,2,\dots,10 \end{cases} \tag{40}$$

The parameters are assumed to be independent and identically distributed following uniform distributions [0.6,1]. In this case, four damage patterns are considered:

- Damage pattern 1: the stiffness of the second storey is reduced by 10%.
- Damage pattern 2: the stiffness of the top storey is reduced by 15%.
- Damage pattern 3: the mass density of the second storey is reduced by 10% and the stiffness of the sixth storey is reduced by 20%.
- Damage pattern 4: the stiffness of the fifth storey is reduced by 15% and the mass density of the top storey is reduced by 25%.

The four damage patterns are investigated to demonstrate the validity and effectiveness of the proposed model updating algorithm in detecting and locating both single and multiple damages. Damage patterns 1 and 2 represent a single damage condition. Damage patterns 3 and 4 represent multiple damage conditions. There is one damage case in pattern 4 that happens in the odd storey, and the updated result is the average of the results of two adjacent substructures.

3.2 Damage localization

This section presents the first step of the proposed surrogate ensemble learning based Bayesian model updating process. After the whole structure is divided into five substructures as Fig. 2 illustrated, ARMAX is used for damage localization. ARMAX model can describe dynamic systems with noise disturbance through its moving-average terms. In order to make the acquired structural excitation and responses retain system characteristics and prevent signal distortion from compromising the damage detection results, no filter is used to pre-process the acquired signals. The motion equation of the first four substructures is written as

$$\begin{aligned} &m_i\ddot{y}_i + (c_i + c_{i+1})\dot{y}_i + (k_i + k_{i+1})y_i \\ &= -m_i\ddot{z}_{i-1} + c_{i+1}\dot{y}_{i+1} + k_{i+1}y_{i+1} \end{aligned} \tag{41}$$

where $\ddot{z}$ and y indicates the absolute acceleration and the inter-storey displacement, and $\ddot{z}_0$ represents the ground acceleration $\ddot{x}_g$. Then introduce the difference expressions

$$\begin{cases} \dot{y}_i = \dfrac{y_i(t+T) - y_i(t-T)}{2T} \\ \ddot{y}_i = \dfrac{y_i(t+T) - 2y_i(t) + y_i(t-T)}{4T^2} \end{cases} \tag{42}$$

where T means the sampling interval. Thus, Eq. (41) can be rewritten as

$$\begin{aligned} &\ddot{y}_i(t) + a_1\ddot{y}_i(t-1) + a_2\ddot{y}_i(t-2) \\ &= b_{11}\ddot{z}_{i-1}(t-1) + b_{12}\ddot{z}_{i-1}(t-2) \\ &\quad + b_{21}\ddot{y}_{i+1}(t-1) + b_{22}\ddot{y}_{i+1}(t-2) + e(t) \end{aligned} \tag{43}$$

where $e(t)$ indicates the prediction error. Eq. (43) can be

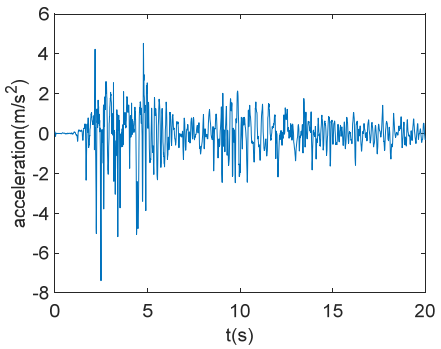

(a) Without noise

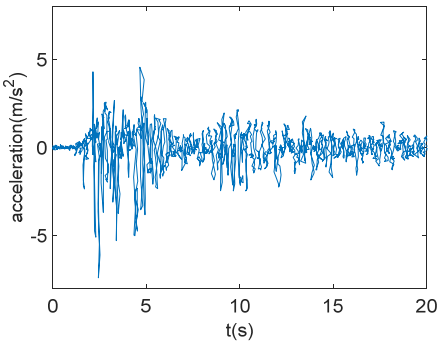

(b) With noise

Fig. 3 Seismic responses

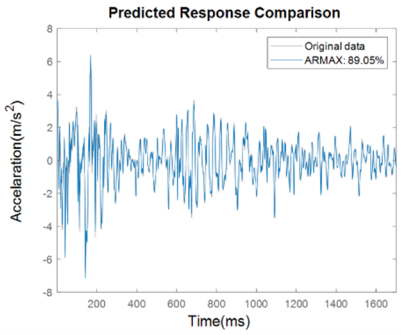

(a) Undamaged: sub 1

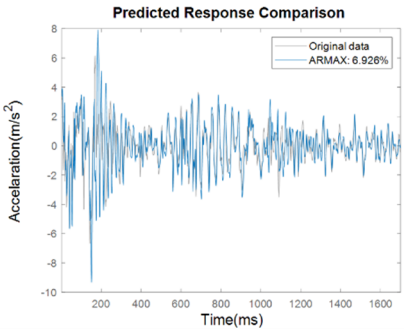

(b) Damaged: sub 1

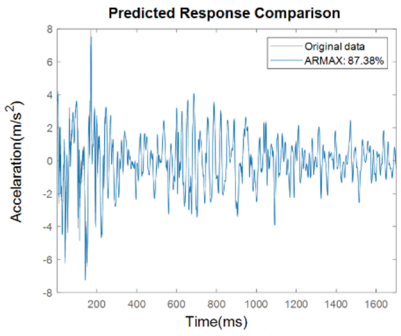

(c) Undamaged: sub 2

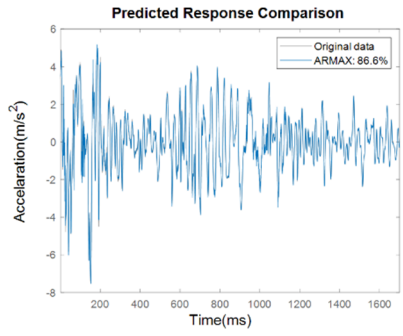

(d) Damaged: sub 2

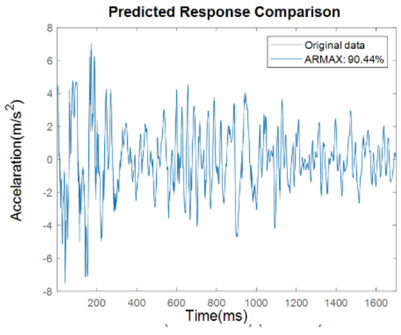

(e) Undamaged: sub 3

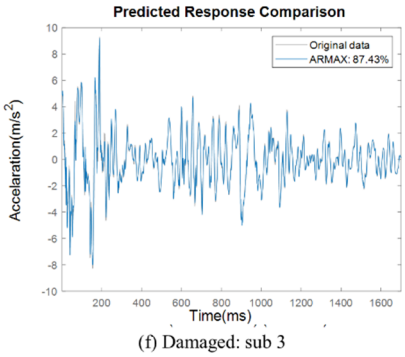

(f) Damaged: sub 3

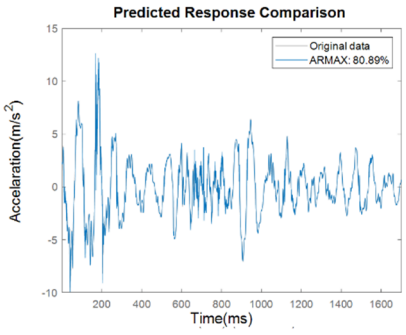

(g) Undamaged: sub 4

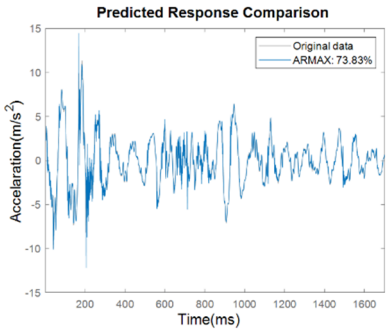

(h) Damaged: sub 4

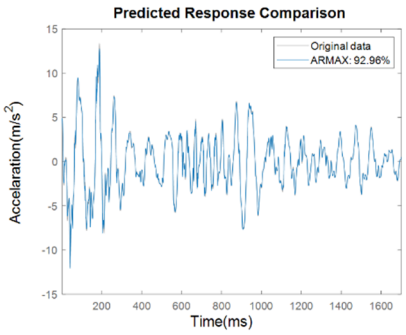

(i) Undamaged: sub 5

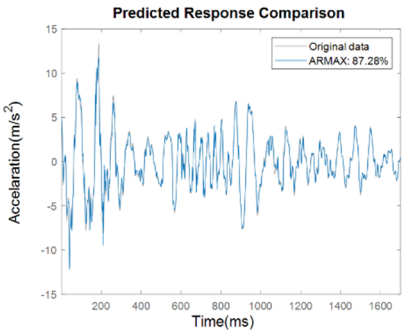

(j) Damaged: sub 5

Fig. 4 Damage localization by ARMAX

regarded as a two-input and single-output ARMAX model. For the top substructure, the motion equation can be formulated as

$$m_n\ddot{y}_i + c_n\dot{y}_n + k_n y_n = -m_n\ddot{z}_{n-1} \tag{44}$$

By substituting Eq. (42), Eq. (44) can be rewritten as

$$\begin{aligned}&\ddot{y}_n(t) + a_1\ddot{y}_n(t-1) + a_2\ddot{y}_n(t-2)\\&= b_1\ddot{z}_{n-1}(t-1) + b_2\ddot{z}_{n-1}(t-2) + e(t)\end{aligned} \tag{45}$$

Eq. (45) can be regarded as a one-input and single-output ARMAX model. Therefore, the ARMAX model can reflect the vibration characteristics of the structure. For the first four substructures, the accelerations of the upper and lower storeys are modeled as the input of the substructure and the acceleration of the middle storey is modeled as the output. For the top substructure, the acceleration of the ninth storey is modeled as the input of substructure and the acceleration of the top storey is modeled as the output. The damage identification process is performed by comparing the NRMSE of the ARMAX models between the undamaged states and the unknown states.

Due to space limitations, this section only uses damage pattern 1 as an example to interpret the damage localization stage. The damage position can be seen from the plot comparing the original observation and the fitted observation as shown in Fig. 4. The NRMSE is marked on the legend. In Fig. 4, The five subplots on the left represent the original undamaged structure, while the subplots on the right denote the damaged structure.

For substructure 1, the NRMSE of undamaged structure and undamaged structure is 89.05% and 6.926%, respectively. It indicates that substructure 1 sustains the damage. For substructures 2-5, the difference of NRMSE between the undamaged structure and the undamaged structure is small, so no damage occurs in the four substructures. Similarly, the damaged substructure under other damage patterns can be identified.

3.3 Feature extraction

Before establishing the surrogate model for each substructure, it is important to apply wavelet packet decomposition technology to extract the features susceptible to structural damage from the acceleration time history recorded by sensors as the output of the metamodels.

To achieve the optimal decomposition effect in wavelet packet decomposition, two factors are crucial: (1) determine the optimal wavelet basis function; (2) Select the appropriate signal decomposition level, that is, the number of layers of wavelet packet decomposition. By choosing the proper wavelet basis for wavelet packet decomposition, a set of feature band coefficients is generated. Only a small number of coefficients can be employed to finish the expression of the original signal when these frequency band coefficients are significantly different. These wavelet bases are referred to as optimum wavelet bases. In order to maximize the energy of wavelet decomposition in the low frequency region and denoising, the wavelet basis function must have a high vanishing moment. This is done mostly utilizing Daubechies (dbN) wavelets (Daubechies 1992). Both the order of the wavelet basis function and decomposition level influence the signal decomposition effect. A method to choose the order of dbN function and the decomposition level is to use l_p norm as the cost function to deal with the above two key problems.

Due to space constraints, this section uses only damage pattern 1 as an illustration of feature extraction. Fig. 4 depicts the l_p norm at various decomposition levels and orders of the dbN function. The l_p norm of wavelet packet decomposition reduces with increasing decomposition level for a given wavelet basis function. When the decomposition level is between 2 and 6, the l_p norm decreases quickly, however, when it is between 6 and 10, it decreases gradually. It can be observed that when the decomposition level is 6, the l_p norm is minimal, ensuring that the representation of structural damage information for each frequency band is acceptable. Table 1 displays the l_p norm of dbN functions of various orders when the decomposition level is 6, with N ranging from 2 to 10. As seen in Table 1,

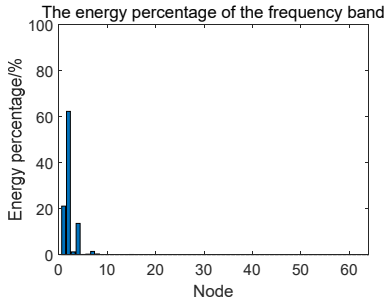

Fig. 5 The frequency band diagram for substructure 1 in damage pattern 1

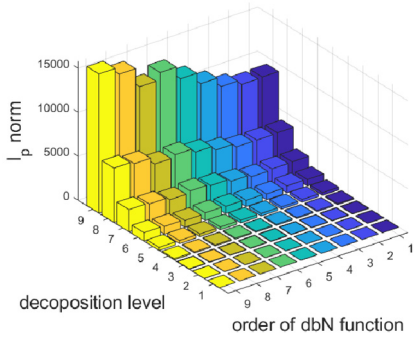

Fig. 6 l_p norm at different decomposition levels and different orders of dbN function

Table 1 The l_p norm of distinct wavelet order N at the decomposition level of 6

Orders	2	3	4	5	6
l_p norm	302.09	307.09	255.40	287.09	313.12
Orders	7	8	9	10	
l_p norm	327.11	306.09	336.27	354.06	

(a) Initial sample (b) Updated sample

Fig. 7 Scatter plot of sample data for substructure 1

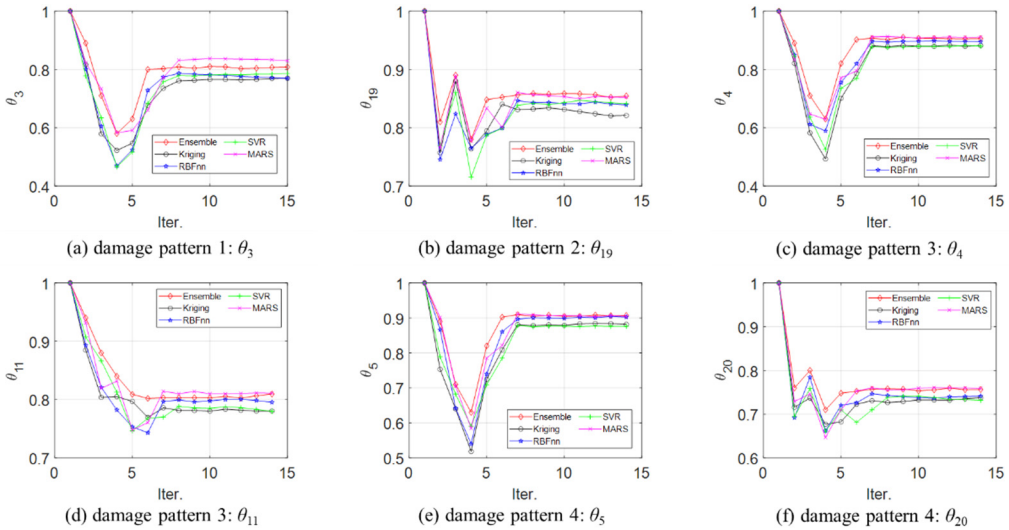

(a) damage pattern 1: θ_3 (b) damage pattern 2: θ_{19} (c) damage pattern 3: θ_4

(d) damage pattern 3: θ_{11} (e) damage pattern 4: θ_5 (f) damage pattern 4: θ_{20}

Fig. 8 Comparison of updated parameters in different models

db4 minimizes the l_p norm; hence, it is the optimal wavelet basis function.

Based on 6-layer wavelet packet decomposition, the decomposition coefficients in each frequency band are reconstructed to obtain the corresponding reconstructed signals, and the wavelet packet energy spectrum method is used to extract the energy value of each reconstructed signal as the signal characteristic information. Fig. 5 depicts the energy percentage of the frequency band for substructure 1 in damage pattern 1. The energy is concentrated in the first four frequency bands, that is, between 0 and 6.25 Hz. After determining the form of the wavelet basis function, the l_p (p is chosen as 1.5 in this study) norm of the node energy is taken as the feature vector, that is, the output of the surrogate model.

3.4 Surrogate ensemble learning based model updating results

After feature extraction, the next step is to build surrogate models. The Latin hypercube sampling (LHS) method are used to create the initial sample space. The sample sizes for the first four substructures and the top substructure are 13 and 9, respectively. To obtain the distribution of the output of each surrogate model, 100 random points were generated by means of the Monte Carlo simulation and used to approximate the PMFs by Eq. (26). Then the PMFs are replaced with PDFs. According to the sample space updating algorithm in Section 2.3, the new points are obtained based on the maximum entropy principle and Bayesian inference, improving the robustness of the surrogate models. After iterations, the sample sizes have reached to 28 and 15.

Take substructure 1 as an example, the scatter plots of sample points of initial and updated sample space are shown in Fig. 7. The newly added points are mainly distributed in the upper right corner of the sample space. Table 2 displays the RMSE of the four surrogate models and ensemble models created for substructure 1 under damage pattern 1 before and after ensemble. It can be observed that SVR, RBFNN and MARS have excellent performance in the initial sample space while Kriging does not. This shows that Kriging performs slightly worse in the case of small samples compared with the other three models. However, after sample space updating, the prediction accuracy of all surrogate models is increased, particularly for the Kriging model, which is sensitive to the sample size. This demonstrates the effectiveness of the sample space updating algorithm based on maximum entropy and Bayesian inference.

To validate the effectiveness and robustness of the probability ensemble method, the individual surrogate models are also carried on the separate Bayesian model updating process. For the ensemble approach and the

Table 2 RMSE of the surrogate models before and after sample space updating

Model	Kriging	SVR	RBFNN	MARS
Initial	0.04633	0.00125	0.00171	0.00129
After updating	0.00080	0.00122	0.00019	0.00117

surrogate models, the trends of updated parameters in the iteration of TMCMC are compared in Fig. 8. It can be observed that all methods converge reasonably fast, and the ensemble approach converges one or two steps earlier than each surrogate model. Besides, four surrogate models are more violent and susceptible than the ensemble approach in

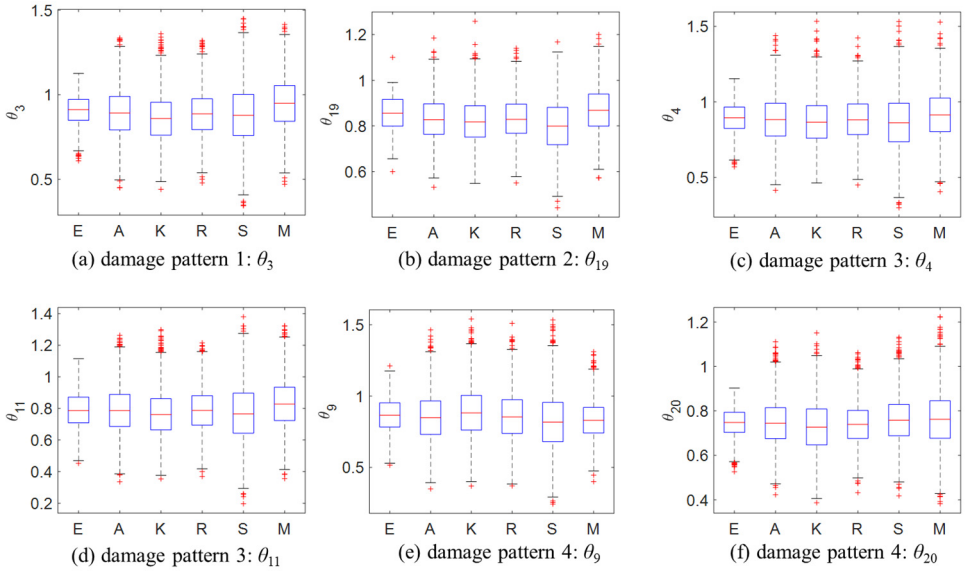

Fig. 9 Comparison of ensemble model and individual surrogate models

Table 3 MPV and variance of the updated parameters in damage pattern 1 (% errors in parenthesis)

Variables	Origin value	Kriging		SVR		RBFNN		MARS		Average model		Ensemble method	
		MPV	Variance	MPV	Variance	MPV	Variance	MPV	Variance	MPV	Variance	MPV	Variance
θ_1	1	0.9342 (-6.58)	0.1745	0.9412 (-5.88)	0.1547	0.9423 (-5.77)	0.2151	0.9425 (-5.75)	0.2045	0.9396 (-6.04)	0.1824	0.9673 (-3.27)	0.1149
θ_2	1	0.9227 (-7.73)	0.1956	0.9114 (-8.86)	0.1765	0.9247 (-7.53)	0.2239	0.9164 (-8.36)	0.2056	0.9182 (-0.818)	0.1969	0.9504 (-4.96)	0.1125
θ_3	0.9	0.8591 (-4.54)	0.1802	0.8609 (-4.34)	0.1665	0.8561 (-3.77)	0.2308	0.9239 (-2.65)	0.1965	0.8724 (-3.07)	0.1892	0.8803 (-2.18)	0.0946
θ_4	1	0.9383 (-6.17)	0.1449	0.9261 (-7.39)	0.1294	0.9326 (-6.74)	0.1824	0.9185 (-8.15)	0.1665	0.9274 (-7.26)	0.1562	0.9612 (-3.88)	0.0981
θ_5	1	0.9214 (-7.86)	0.1512	0.9096 (-9.04)	0.1298	0.9154 (-8.46)	0.1963	0.9236 (-7.64)	0.1782	0.9189 (-8.11)	0.1442	0.9609 (-3.91)	0.1046
θ_6	1	0.9326 (-6.74)	0.1646	0.9163 (-8.37)	0.1414	0.9249 (-7.51)	0.2076	0.9086 (-9.14)	0.1876	0.9207 (-7.93)	0.1806	0.9523 (-4.77)	0.1053

Table 4 MPV and variance of the updated parameters in damage pattern 2 (% errors in parenthesis)

Variables	Origin value	Kriging		SVR		RBFNN		MARS		Average model		Ensemble method	
		MPV	Variance	MPV	Variance	MPV	Variance	MPV	Variance	MPV	Variance	MPV	Variance
θ_{17}	1	0.9325 (-6.75)	0.1338	0.9278 (-7.22)	0.1465	0.9513 (-4.87)	0.1793	0.9295 (-7.05)	0.2002	0.9316 (-6.84)	0.1614	0.9820 (-1.80)	0.099
θ_{18}	1	0.9342 (-6.58)	0.1179	0.9264 (-7.36)	0.1325	0.9317 (-6.83)	0.1621	0.9074 (-9.16)	0.1476	0.9191 (-8.09)	0.1369	0.9801 (-1.99)	0.0881
θ_{19}	0.85	0.8158 (-4.02)	0.1008	0.8216 (-3.34)	0.1142	0.7963 (-6.32)	0.1608	0.8649 (1.75)	0.1495	0.8317 (-2.15)	0.1264	0.8533 (0.39)	0.0954
θ_{20}	1	0.9275 (-7.25)	0.1278	0.9308 (-6.92)	0.1306	0.9326 (-6.74)	0.1657	0.9185 (-8.15)	0.1426	0.9274 (-7.26)	0.1372	0.9736 (-2.64)	0.1002

Table 5 MPV and variance of the updated parameters in damage pattern 3 (% errors in parenthesis).

Variables	Origin value	Kriging		SVR		RBFNN		MARS		Average model		Ensemble method	
		MPV	Variance	MPV	Variance	MPV	Variance	MPV	Variance	MPV	Variance	MPV	Variance
θ_1	1	0.9504 (-4.96)	0.2186	0.9456 (-5.44)	0.2676	0.9488 (-5.12)	0.1895	0.9673 (-3.27)	0.2302	0.9517 (-4.83)	0.2042	0.9881 (-1.19)	0.1152
θ_2	1	0.9331 (-6.69)	0.2284	0.9421 (-5.79)	0.2301	0.9187 (-8.13)	0.1872	0.9165 (-8.35)	0.2073	0.9331 (-6.69)	0.2284	0.9582 (-4.18)	0.1107
θ_3	1	0.9437 (-5.63)	0.1301	0.9381 (-6.19)	0.1798	0.9402 (-5.98)	0.1426	0.9524 (4.76)	0.1641	0.9412 (-5.88)	0.1538	0.9902 (-0.98)	0.1029
θ_4	0.9	0.8629 (-4.12)	0.1886	0.8738 (-2.91)	0.1802	0.8567 (-4.81)	0.2128	0.8718 (-3.13)	0.1984	0.8689 (-3.45)	0.1801	0.8937 (-0.7)	0.1023
θ_5	1	0.9380 (-6.20)	0.1448	0.9419 (-5.81)	0.2173	0.9302 (-6.98)	0.1634	0.9103 (-8.97)	0.1942	0.9347 (-6.53)	0.1857	0.9875 (-1.25)	0.1131
θ_6	1	0.9344 (-6.56)	0.1397	0.9149 (-8.51)	0.2055	0.9208 (-7.92)	0.1538	0.9437 (-5.63)	0.1889	0.9289 (-7.11)	0.1924	0.9804 (-1.96)	0.1126
θ_9	1	0.9837 (-1.63)	0.1319	0.9614 (-3.86)	0.2014	0.9531 (-4.69)	0.1549	0.9429 (-5.71)	0.1735	0.9597 (-4.03)	0.1687	0.9842 (-1.58)	0.1152
θ_{10}	1	0.9833 (-1.67)	0.1149	0.9501 (-4.99)	0.2134	0.9243 (-7.57)	0.1426	0.9435 (-5.65)	0.1648	0.9602 (-3.98)	0.1702	0.9826 (-1.74)	0.1107
θ_{11}	0.8	0.8142 (1.77)	0.1341	0.7797 (-2.54)	0.1902	0.8205 (2.56)	0.1498	0.8327 (4.09)	0.1637	0.8189 (2.36)	0.1586	0.7850 (-1.88)	0.1029
θ_{12}	1	0.9817 (-1.83)	0.1120	0.9546 (-4.54)	0.2123	0.9624 (-3.76)	0.1533	0.9322 (-6.78)	0.1877	0.9644 (-3.56)	0.1706	0.9813 (-1.87)	0.1023
θ_{13}	1	0.9692 (-3.08)	0.1216	0.9492 (-5.08)	0.1987	0.9506 (-4.94)	0.1324	0.9433 (-5.67)	0.1655	0.9744 (-2.56)	0.1521	0.9796 (-2.04)	0.1131
θ_{14}	1	0.9929 (-0.71)	0.1144	0.9601 (-3.99)	0.1877	0.9542 (-4.58)	0.1364	0.9488 (-5.12)	0.1511	0.9675 (-3.25)	0.1244	0.9930 (-0.70)	0.1126

the initial steps. A conclusion can be drawn that EOS based model updating is superior to individual surrogate model based model updating in terms of convergence speed.

Fig. 9 displays the boxplots of the updating parameters for the damage position under the four damage patterns. The boxplots include the ensemble model, four individual models, and their weighted average. In the weighted average model, the weight assigned to each individual model is determined based on the reciprocal error observed during the training phase. Results of different models under four damage patterns are separated to investigate the effect of the ensemble approach on the predictive accuracy and uncertainties. Notably, when the ensemble approach is employed, the spread of variables is narrower, indicating reduced parameter uncertainty. In the boxplots, outliers are represented by points outside the upper and lower lines and are plotted separately. The boxplots for the individual surrogate models exhibit several outliers, whereas the boxplot for the ensemble approach contains only a few outliers. These observations highlight the promotion of the ensemble approach to mitigate uncertainties associated with the surrogate models. Furthermore, it underscores the advantages of the proposed EOS approach over traditional weighted-based EOS methods, as the weighted average approach may be inferior to the best individual model. Conversely, the proposed EOS approach yields smaller uncertainties compared to all individual surrogate models.

The Kriging model is taken as a reference compared to the ensemble model for subsequent analysis. The most probable value (MPV) and the variance in four damage patterns are presented in Tables 3 to 6. It is seen that updated parameters for the four damage patterns have been well identified and the structural damage can be quantified. The errors of MPV for the four surrogate models are all within 10% in the four damage patterns, while that for the ensemble model are within 5%. The updated errors and variances, associated with the weighted average model, have also been incorporated in Tables 3-6. The results indicate that the weighted average model performs moderately in terms of mean prediction value (MPV) and variance, while the ensemble model clearly outperforms the individual models and the weighted average model due to the sample space updating. In addition, the posterior variances of parameters are also shown in Tables 3 to 6., which can be used to provide uncertainty quantification for the inferred damage for each substructure. Upon examining the results, it becomes evident that the majority of posterior variances obtained through the ensemble approach are below 0.12. Conversely, for the individual models, the variances are considerably larger. Notably, for damage patterns 3 and 4, the variances of certain parameters in the individual models are approximately twice as large as those observed in the ensemble approach.

Figs. 6 to 9 show the marginal posterior PDFs of the parameters of the damaged substructure obtained by the Kriging model and ensemble approach under the four

Table 6 MPV and variance of the updated parameters in damage pattern 4 (% errors in parenthesis)

Variables	Origin value	Kriging		SVR		RBFNN		MARS		Average model		Ensemble method	
		MPV	Variance	MPV	Variance	MPV	Variance	MPV	Variance	MPV	Variance	MPV	Variance
θ_5	1	0.9434 (-5.66)	0.2332	0.9458 (-5.42)	0.2565	0.9533 (-4.67)	0.1823	0.9495 (-5.05)	0.2132	0.9486 (-5.14)	0.1742	0.9758 (-2.42)	0.1229
θ_6	1	0.9476 (-5.24)	0.2256	0.9354 (-6.46)	0.1463	0.9347 (-6.53)	0.1531	0.9574 (-4.26)	0.1866	0.9491 (-5.09)	0.1569	0.9792 (-2.08)	0.1205
θ_7	1	0.9104 (-8.96)	0.1379	0.9216 (-7.84)	0.1942	0.9363 (-6.37)	0.1608	0.9549 (-4.51)	0.1595	0.9417 (-5.83)	0.1454	0.9571 (-4.29)	0.1082
θ_8	1	0.9361 (-6.39)	0.1429	0.9508 (-4.92)	0.1906	0.9436 (-5.64)	0.1657	0.9385 (-6.15)	0.1726	0.9374 (-6.26)	0.1532	0.9814 (-1.86)	0.1178
θ_9	0.85	0.8200 (-3.53)	0.2018	0.8158 (-4.02)	0.1708	0.8649 (1.75)	0.1142	0.7963 (-6.32)	0.1608	0.8216 (-3.34)	0.1495	0.8317 (-2.15)	0.1264
θ_{10}	1	0.9363 (-6.37)	0.1296	0.9295 (-7.05)	0.1938	0.9368 (-6.32)	0.1126	0.9696 (-3.04)	0.1857	0.9415 (-5.85)	0.1426	0.9274 (-7.26)	0.1372
θ_{11}	1	0.9437 (-5.63)	0.2054	0.9489 (-5.11)	0.1873	0.9332 (-6.68)	0.1634	0.9383 (-6.17)	0.1942	0.9407 (-5.93)	0.1857	0.9814 (-1.86)	0.0998
θ_{12}	1	0.9524 (-4.76)	0.2166	0.9259 (-7.41)	0.2302	0.9408 (-5.92)	0.1648	0.9517 (-4.83)	0.1814	0.9339 (-6.61)	0.1711	0.9769 (-2.31)	0.0972
θ_{13}	1	0.9379 (-6.21)	0.1786	0.9524 (-4.76)	0.1914	0.9431 (-569)	0.1439	0.9507 (-4.93)	0.1615	0.9497 (-5.03)	0.1512	0.9807 (-1.93)	0.1013
θ_{14}	1	0.9468 (-5.32)	0.1943	0.9446 (-5.54)	0.2102	0.9343 (-6.57)	0.1536	0.9635 (-3.65)	0.1548	0.9501 (-4.99)	0.1769	0.9783 (-2.17)	0.1065
θ_{17}	1	0.9533 (-4.67)	0.1308	0.9604 (-3.96)	0.2086	0.9416 (-5.84)	0.2116	0.9608 (-3.92)	0.1495	0.9623 (-3.77)	0.1902	0.9924 (-0.76)	0.0691
θ_{18}	1	0.9383 (-6.17)	0.1031	0.9331 (-6.69)	0.2284	0.9421 (-5.79)	0.2301	0.9187 (-8.13)	0.1872	0.9165 (-8.35)	0.2073	0.9800 (-2.00)	0.0652
θ_{19}	1	0.9378 (-6.22)	0.1027	0.9437 (-5.63)	0.1301	0.9381 (-6.19)	0.1798	0.9402 (-5.98)	0.1426	0.9524 (4.76)	0.1641	0.9792 (-2.08)	0.0644
θ_{20}	0.75	0.7299 (-2.68)	0.1153	0.7137 (-4.84)	0.1688	0.7281 (-2.92)	0.1476	0.7102 (-5.31)	0.1201	0.7224 (3.68)	0.1641	0.7349 (-2.02)	0.0640

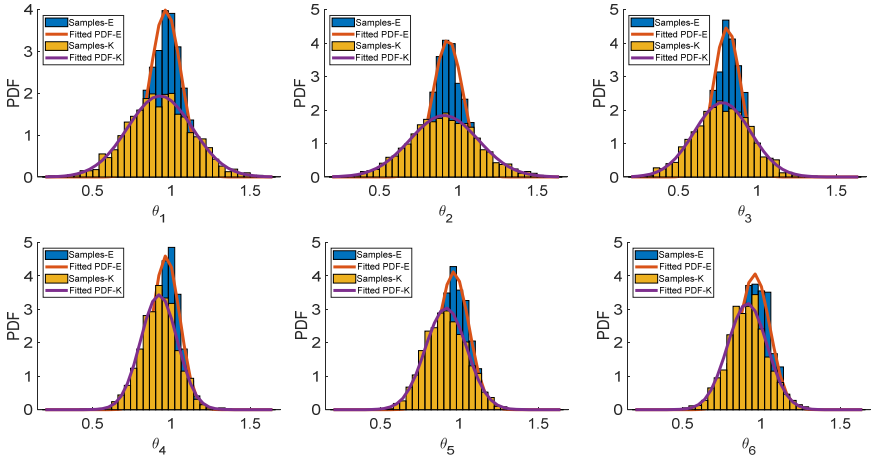

Fig. 10 Updated parameters in damage pattern 1

damage patterns. It is evident that when the ensemble approach is employed, the spread of the updated parameters is reduced, confirming the consistent conclusion obtained from the boxplots.

From observations in Tables 3-6 and Figs. 6-9, it can be concluded that the proposed three-step surrogate ensemble learning model updating method effectively enables parameter identification and damage quantification. In terms of both mean prediction value (MPV) and posterior variances, the EOS-based model updating outperforms

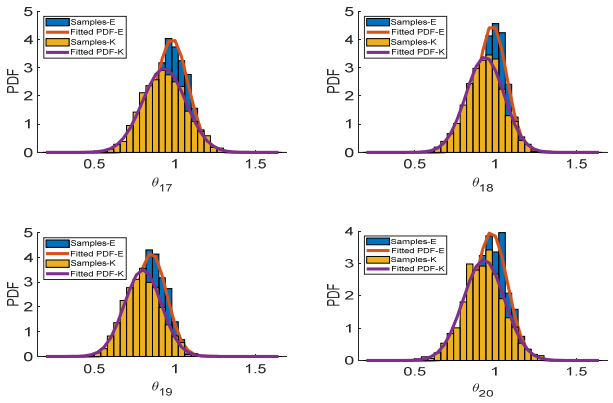

Fig. 11 Updated parameters in damage pattern 2

individual surrogate model-based updating for all damage patterns. This also highlights the advantage of the probability ensemble approach over traditional EOS methods based on the weighted average, which tends to yield inferior results compared to the best individual model.

4. Case study-shaking table experiment

The proposed method is also implemented in a shaking table experiment of a 3-storey reinforced concrete building structure. The test specimen, depicted in Fig. 14, has a plan dimension of 5140 mm (x direction) by 4300 mm (y direction) and a total height of 7340 mm. The masses of the three storey structures are 15.51 t, 15.32 t, and 14.66 t, respectively. The dynamic response of the structure is obtained by utilizing the strong zero-mean motion records known as JMA Kobe. The JMA Kobe records were employed with the seismic motions scaled to peak ground accelerations of 0.07 g, representing the service level earthquake for the RC structure. It is important to note that the specimen was uniaxially loaded either in the x or y direction exclusively.

The proposed method is also implemented in a shaking table experiment of a 3-storey reinforced concrete building structure. The test specimen, depicted in Fig. 14, has a plan dimension of 5140 mm (x direction) by 4300 mm (y direction) and a total height of 7340 mm. The masses of the three storey structures are 15.51 t, 15.32 t, and 14.66 t, respectively. The dynamic response of the structure is obtained by utilizing the strong zero-mean motion records known as JMA Kobe. The JMA Kobe records were employed with the seismic motions scaled to peak ground accelerations of 0.07 g, representing the service level earthquake for the RC structure. It is important to note that the specimen was uniaxially loaded either in the x or y direction exclusively.

5. Conclusions

A novel three-step Bayesian model updating framework suitable for the model updating and damage identification is presented in this paper. First, the substructure division and ARMAX time series analysis are employed to identify the damage localization. Then the sample space updating algorithm is used to construct a series of accurate and robust

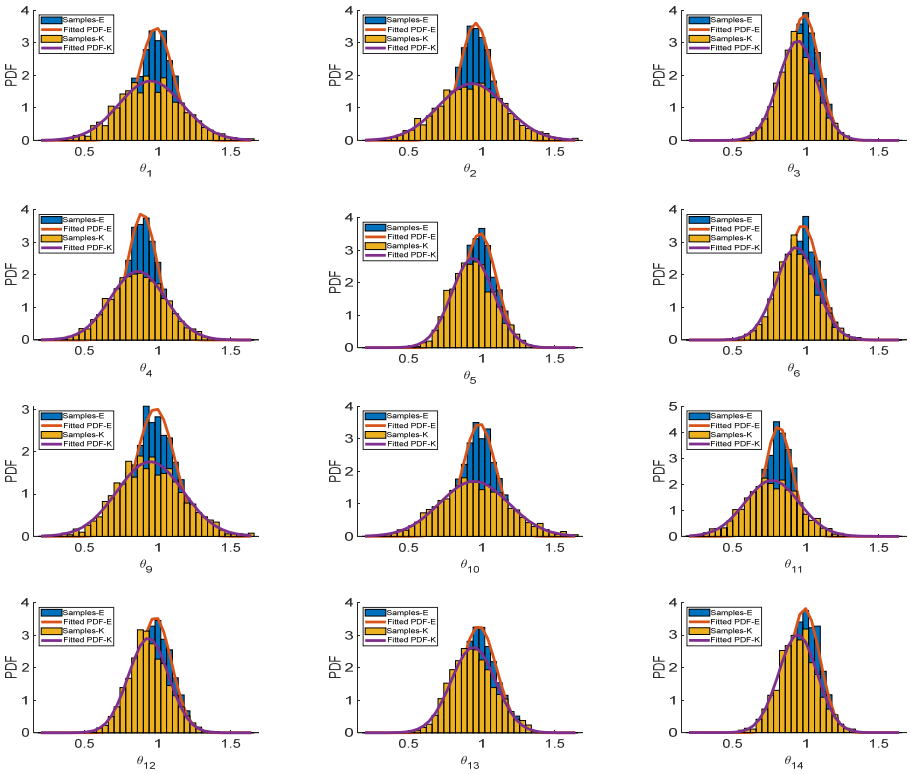

Fig. 12 Updated parameters in damage pattern 3

Table 7 MPV and variance of the updated parameters

Seismic direction	Variables	Reference data	Average model		Ensemble method	
			MPV	variance	MPV	variance
x direction	θx_1	0.9079	0.8756	0.1354	0.9022	0.1098
	θx_2	0.9197	0.9382	0.1479	0.8804	0.1121
	θx_3	0.9424	0.9124	0.1236	0.9303	0.0978
y direction	θy_1	0.9147	0.9474	0.1372	0.9212	0.0992
	θy_2	0.9428	0.9087	0.1592	0.9309	0.1023
	θy_3	0.8926	0.9245	0.1603	0.9173	0.1088

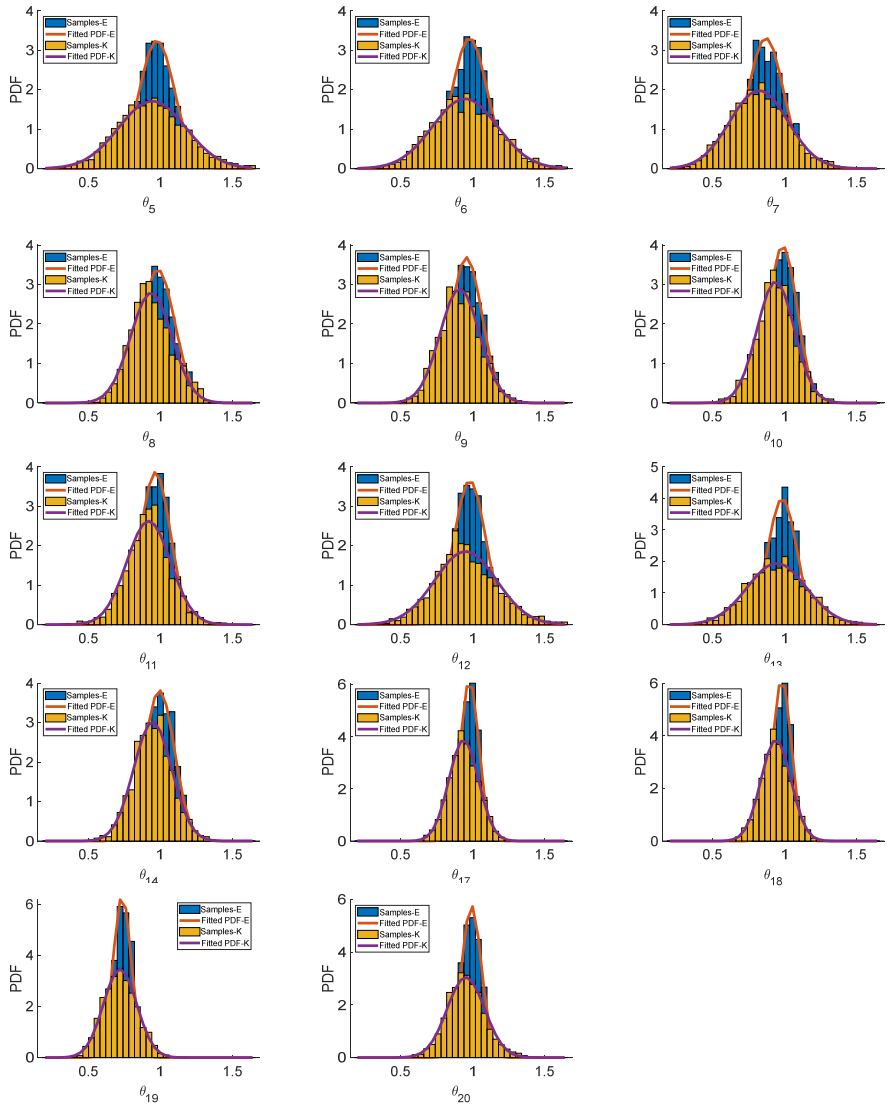

Fig. 13 Updated parameters in damage pattern 4

surrogate models. Finally, the posterior PDFs of individual surrogate models are fused by the probability ensemble approach. The developed framework of surrogate ensemble learning based model updating is demonstrated in a ten-storey frame and a shaking table experiment. The structure is investigated to verify and validate the accuracy and effectiveness of the proposed framework. The main findings of this study could be summarised as follows:

- Damage localization based on substructure division and ARMAX provides an efficient dimensionality reduction technique.
- The sample space updating algorithm can enhance the surrogate models.
- The model updating and damage identification can be well implemented on the proposed Bayesian

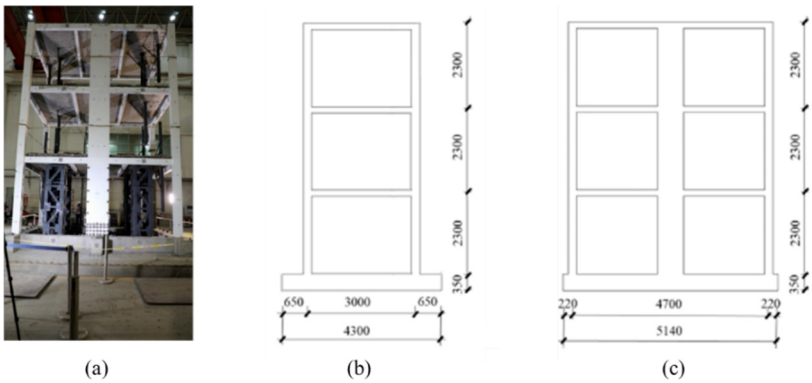

Fig. 14 Shaking table experiment: (a) Test specimen; (b) Side view in x direction; (c) Side view in y direction

model updating framework.

- The surrogate ensemble learning based model updating outperforms in both MPV and posterior variances compared to individual surrogate model based updating. Compared with the existing EOS methods which always have worse results than the best individual model, the EOS framework is obviously better in uncertainty quantification due to the consideration of probability ensemble.

Acknowledgments

The authors gratefully acknowledge the financial support from the Scientific Research Fund of the Institute of Engineering Mechanics, China Earthquake Administration (Grant No. 2021D18), Visiting Researcher Fund Program of State Key Laboratory of Water Resources and Hydropower Engineering Science (2021SGG01), and Scientific Research Fund of Multi-Functional Shaking Tables Laboratory of Beijing University of Civil Engineering and Architecture.

References

Abbasnia, R., Mirzaee, A. and Shayanfar, M. (2018), "Simultaneous identification of damage in bridge under moving mass by Adjoint variable method", *Smart Struct. Syst., Int. J.*, **21**(4), 449-467. https://doi.org/10.12989/sss.2018.21.4.449

Adnan, R.M., Liang, Z.M., Heddam, S., Zounemat-Kermani, M., Kisi, O. and Li, B.Q. (2020), "Least square support vector machine and multivariate adaptive regression splines for streamflow prediction in mountainous basin using hydro-meteorological data as inputs", *J. Hydrol.*, **586**, 124371. https://doi.org/10.1016/j.jhydrol.2019.124371.

Alabi, S.A., Hu, Q., Lam, H.F. and Zhu, H.P. (2018), "Bayesian ballast damage detection utilizing a modified evolutionary algorithm", *Smart Struct. Syst., Int. J.*, **21**(4), 435-448. https://doi.org/10.12989/sss.2018.21.4.435

Alexander, I., Andras, S. and Andy, J. (2008), *Engineering design via surrogate modelling*, University Southampton, Southampton, UK.

Alizadeh, R., Jia, L.Y., Nellippallil, A.B., Wang, G.X., Hao, J., Allen, J.K. and Mistree, F. (2019), "Ensemble of surrogates and cross-validation for rapid and accurate predictions using small data sets", *Ai Edam-Artificial Intelligence for Engineering Design Analysis and Manufacturing*, **33**(4), 484-501. https://doi.org/10.1017/S089006041900026X

Alkayem, N.F., Cao, M.S., Zhang, Y.F., Bayat, M. and Su, Z.Q. (2018), "Structural damage detection using finite element model updating with evolutionary algorithms: a survey", *Neural Comput. Applicat.*, **30**(2), 389-411. http://doi.org/10.1007/s00521-017-3284-1

Azim, M.R., Zhang, H.Y. and Gul, M. (2020), "Damage detection of railway bridges using operational vibration data: theory and experimental verifications", *Struct. Monitor. Maint., Int. J.*, **7**(2), 149-166. http://doi.org/10.12989/smm.2020.7.2.149

Barazanchy, D., Martinez, M., Rocha, B. and Yanishevsky, M. (2014), "A hybrid structural health monitoring system for the detection and localization of damage in composite structures", *J. Sensors*, **2014**, 1-10. https://doi.org/10.1155/2014/109403

Beck, J.L. and Katafygiotis, L.S. (1998), "Updating models and their uncertainties. I: Bayesian statistical framework", *J. Eng. Mech.*, **124**(4), 455-461. http://doi.org/Doi 10.1061/(Asce)0733-9399(1998)124:4(455)

Beniddir, M.A., Kang, K.B., Genta-Jouve, G., Huber, F., Rogers, S. and van der Hooft, J.J.J. (2021), "Advances in decomposing complex metabolite mixtures using substructure- and network-based computational metabolomics approaches", *Natural Product Reports*, **38**(11), 1967-1993. http://doi.org/10.1039/d1np00023c

Berk, J., Nguyen, V., Gupta, S., Rana, S. and Venkatesh, S. (2018), "Exploration enhanced expected improvement for bayesian optimization", *Proceedings of the Joint European Conference on Machine Learning and Knowledge Discovery in Databases*.

Bisbo, M.K. and Hammer, B. (2020), "Efficient global structure optimization with a machine-learned surrogate model", *Phys. Rev. Lett.*, **124**(8), 086102. http://doi.org/10.1103/PhysRevLett.124.086102

Cai, E.J. and Zhang, Y. (2022), "Gaussian mixture model based phase prior learning for video motion estimation", *Mech. Syst. Signal Process.*, **175**. https://doi.org/10.1016/j.ymssp.2022.109103.

Candy, J.V. (2005), *Model-based signal processing*, John Wiley & Sons.

Chen, Y.-T., Shi, J., Ye, Z., Mertz, C., Ramanan, D. and Kong, S. (2022), "Multimodal object detection via probabilistic ensembling", *Proceedings of the Computer Vision–ECCV 2022: 17th European Conference*, Tel Aviv, Israel, October.

Cheng, K. and Lu, Z.Z. (2020), "Structural reliability analysis based on ensemble learning of surrogate models", *Struct. Safety*, **83**, 101905. https://doi.org/10.1016/j.strusafe.2019.101905

Cheung, S.H. and Beck, J.L. (2009), "Bayesian model updating using hybrid Monte Carlo simulation with application to structural dynamic models with many uncertain parameters", *J. Eng. Mech.*, **135**(4), 243-255. http://doi.org/10.1061/(Asce)0733-9399(2009)135:4(243)

Ching, J. and Beck, J.L. (2003), Two-Stage Bayesian Structural Health Monitoring Approach for Phase II ASCE Experimental Benchmark Studies.

Ching, J.Y. and Chen, Y.C. (2007), "Transitional markov chain monte carlo method for Bayesian model updating, model class selection, and model averaging", *J. Eng. Mech.*, **133**(7), 816-832. http://doi.org/10.1061/(Asce)0733-9399(2007)133:7(816)

Christelis, V., Kopsiaftis, G. and Mantoglou, A. (2019), "Performance comparison of multiple and single surrogate models for pumping optimization of coastal aquifers", *Hydrol. Sci. J.*, **64**(3), 336-349. https://doi.org/10.1080/02626667.2019.1584400

Collins, J.D., Hart, G.C., Hasselman, T.K. and Kennedy, B. (1974), "Statistical Identification of Structures", *AIAA J.*, **12**(2), 185-190. http://doi.org/Doi 10.2514/3.49190

Daubechies, I. (1992), Ten lectures on wavelets: SIAM.

DeVore, C., Jiang, Z.S., Christenson, R.E., Stromquist-LeVoir, G. and Johnson, E.A. (2016), "Experimental verification of substructure identification for damage detection in shear buildings", *J. Eng. Mech.*, **142**(1), 04015060. https://doi.org/10.1061/(ASCE)EM.1943-7889.0000929

Dhamotharan, V., Jadhav, P.D., Ramu, P. and Prakash, A.K. (2018), "Optimal design of savonius wind turbines using ensemble of surrogates and CFD analysis", *Struct. Multidiscipl. Optimiz.*, **58**(6), 2711-2726. http://doi.org/10.1007/s00158-018-2052-x

Ding, Y., Ren, P., Zhao, H. and Miao, C. (2018), "Structural health monitoring of a high-speed railway bridge: five years review and lessons learned", *Smart Struct. Syst., Int. J.*, **21**(5), 695-703. https://doi.org/10.12989/sss.2018.21.5.695

Do, N.T., Mei, Q.P. and Gul, M. (2019), "Damage assessment of shear-type structures under varying mass effects", *Struct. Monitor. Maint., Int. J.*, **6**(3), 237-254. http://doi.org/10.12989/smm.2019.6.3.237

Effendi, M.R., Mengko, T.L.R., Gunawan, A.H. and Munir, A. (2019), "Performance evaluation of wavelet packet modulation for wireless digital communications", *Proceedings of the International Symposium on Networks, Computers and Communications* (*ISNCC*), Istanbul, Turkey.

Elias, I., Rubio, J.D., Martinez, D.I., Vargas, T.M., Garcia, V., Mujica-Vargas, D., Meda-Campana, J.A., Pacheco, J., Gutierrez, G.J. and Zacarias, A. (2020), "Genetic algorithm with radial basis mapping network for the electricity consumption modeling", *Appl. Sci.-Basel*, **10**(12), 4239. https://doi.org/10.3390/app10124239.

Erazo, K. and Hernandez, E.M. (2016), "Bayesian model–data fusion for mechanistic postearthquake damage assessment of building structures", *J. Eng. Mech.*, **142**(9), 04016062. https://doi.org/10.1061/(ASCE)EM.1943-7889.0001114

Fei, J. and Wang, T. (2019), "Adaptive fuzzy-neural-network based on RBFNN control for active power filter", *Int. J. Mach. Learn. Cybernet.*, **10**, 1139-1150. https://doi.org/10.1007/s13042-018-0792-y

Flah, M., Nunez, I., Ben Chaabene, W. and Nehdi, M.L. (2021), "Machine learning algorithms in civil structural health monitoring: a systematic review", *Arch. Computat. Methods Eng.*, **28**(4), 2621-2643. https://doi.org/10.1007/s11831-020-09471-9

Friedman, J.H. (1991), "Multivariate adaptive regression splines", *The Annals of Statistics*, **19**(1), 1-67. https://doi.org/10.1214/aos/1176347963

Goel, T., Haftka, R.T., Shyy, W. and Queipo, N.V. (2007), "Ensemble of surrogates", *Struct. Multidiscipl. Optimiz.*, **33**(3), 199-216. http://doi.org/10.1007/s00158-006-0051-9

Güemes, A., Fernandez-Lopez, A., Pozo, A.R. and Sierra-Pérez, J. (2020), "Structural health monitoring for advanced composite structures: a review", *J. Compos. Sci.*, **4**(1), 13. https://doi.org/10.3390/jcs4010013

He, W.Y., Zhu, S. and Ren, W.X. (2018), "Progressive damage detection of thin plate structures using wavelet finite element model updating", *Smart Struct. Syst., Int. J.*, **22**(3), 277-290. https://doi.org/10.12989/sss.2018.22.3.277

Hoa, T.N., Khatir, S., Roeck, G.D., Long, N.N., Thanh, B.T. and Wahab, M.A. (2020), "An efficient approach for model updating of a large-scale cable-stayed bridge using ambient vibration measurements combined with a hybrid metaheuristic search algorithm", *Smart Struct. Syst., Int. J.*, **25**(4), 487-499. https://doi.org/10.12989/sss.2020.25.4.487

Hou, R. and Xia, Y. (2020), "Review on the new development of vibration-based damage identification for civil engineering structures: 2010-2019", *J. Sound Vib.*, **491**(9). https://doi.org/10.1016/j.jsv.2020.115741

Houret, T., Besnier, P., Vauchamp, S. and Pouliguen, P. (2019), "Controlled stratification based on kriging surrogate model: An algorithm for determining extreme quantiles in electromagnetic compatibility risk analysis", *IEEE Access*, **8**, 3837-3847. https://doi.org/10.1109/ACCESS.2019.2961851

Hu, J. and Yang, J.H. (2018), "Operational modal analysis and Bayesian model updating of a coupled building", *Int. J. Struct. Stabil. Dyn.*, **19**(01), p. 1940012. https://doi.org/10.1142/S0219455419400121

Huang, M.S., Cheng, X.H. and Lei, Y.Z. (2021), "Structural damage identification based on substructure method and improved whale optimization algorithm", *J. Civil Struct. Health Monitor.*, **11**(2), 351-380. http://doi.org/10.1007/s13349-020-00456-7

Jiang, S.H., Papaioannou, I. and Straub, D. (2018), "Bayesian updating of slope reliability in spatially variable soils with in-situ measurements", *Eng. Geol.*, **239**, 310-320. http://doi.org/10.1016/j.enggeo.2018.03.021

Jiang, P., Zhou, Q. and Shao, X. (2020), *Surrogate model-based engineering design and optimization*, Springer.

Khatir, S., Wahab, M.A., Boutchicha, D. and Khatir, T. (2019), "Structural health monitoring using modal strain energy damage indicator coupled with teaching-learning-based optimization algorithm and isogoemetric analysis", *J. Sound Vib.*, **448**, 230-246. http://doi.org/10.1016/j.jsv.2019.02.017

Kirschner, J., Mutny, M., Hiller, N., Ischebeck, R. and Krause, A. (2019), "Adaptive and safe Bayesian optimization in high dimensions via one-dimensional subspaces", *Proceedings of the International Conference on Machine Learning*.

Krige, D.G. (1951), "A statistical approach to some basic mine valuation problems on the Witwatersrand", *J. Southern African Inst. Min. Metall.*, **52**(6), 119-139. https://hdl.handle.net/10520/AJA0038223X_4792

Krishansamy, L. and Arumulla, R. (2018), "A hybrid structural health monitoring technique for detection of subtle structural damage", *Smart Struct. Syst., Int. J.*, **22**(5), 587-609. https://doi.org/10.12989/sss.2018.22.5.587

Kwag, S. and Gupta, A. (2018), "Computationally efficient fragility assessment using equivalent elastic limit state and Bayesian updating", *Comput. Struct.*, **197**, 1-11. http://doi.org/10.1016/j.compstruc.2017.11.011

Li, J. and Hao, H. (2014), "Substructure damage identification based on wavelet-domain response reconstruction", *Struct. Health Monitor., Int. J.*, **13**(4), 389-405. http://doi.org/10.1177/1475921714532991

Li, X., Gong, C.L., Gu, L.X., Gao, W.K., Jing, Z. and Su, H. (2018), "A sequential surrogate method for reliability analysis based on radial basis function", *Struct. Safety*, **73**, 42-53. http://doi.org/10.1016/j.strusafe.2018.02.005

Li, C., Li, H. and Chen, X. (2021), "A framework for fast estimation of structural seismic responses using ensemble machine learning model", *Smart Struct. Syst., Int. J.*, **28**(3), 425-

441. https://doi.org/10.12989/sss.2021.28.3.425
Liao, X., Sun, J., Wang, Y. and Li, M. (2021), "Damage detection based on multi-wavelet basis and multi-scale feature fusion", *Proceedings of 2021 International Conference on Machine Learning and Intelligent Systems Engineering* (*MLISE*), pp. 210-213. http://doi.org/10.1109/mlise54096.2021.00044
Lin, G.W., Zhang, Y. and Liao, Q.Z. (2021), "Developing efficient model updating approaches for different structural complexity-an ensemble learning and uncertainty quantifications", *Smart Struct. Syst.*, *Int. J.*, **29**(2), 321-336. http://doi.org/10.12989/sss.2022.29.2.321
Liu, L., Mi, J., Zhang, Y. and Lei, Y. (2021), "Damage detection of bridge structures under unknown seismic excitations using support vector machine based on transmissibility function and wavelet packet energy", *Smart Struct. Syst.*, *Int. J.*, **27**(2), 257-266. https://doi.org/10.12989/sss.2021.27.2.257
Lo, M.K. and Leung, Y.F. (2019), "Bayesian updating of subsurface spatial variability for improved prediction of braced excavation response", *Can. Geotech. J.*, **56**(8), 1169-1183. http://doi.org/10.1139/cgj-2018-0409
Mao, J.X., Wang, H. and Spencer, B.F. (2019), "Gaussian mixture model for automated tracking of modal parameters of long-span bridge", *Smart Struct. Syst.*, *Int. J.*, **24**(2), 243-256. https://doi.org/10.12989/sss.2019.24.2.243
Mao, J.X., Wang, H. and Li, J. (2020), "Bayesian Finite Element Model Updating of a Long-Span Suspension Bridge Utilizing Hybrid Monte Carlo Simulation and Kriging Predictor", *KSCE J. Civil Eng.*, **24**(2), 569-579. http://doi.org/10.1007/s12205-020-0983-4
Martino, L. (2018), "A review of multiple try MCMC algorithms for signal processing", *Digital Signal Process.*, **75**, 134-152. http://doi.org/10.1016/j.dsp.2018.01.004
Mei, L., Li, H., Zhou, Y., Wang, W. and Xing, F. (2019), "Substructural damage detection in shear structures via ARMAX model and optimal subpattern assignment distance", *Eng. Struct.*, **191**(JUL.15), 625-639. https://doi.org/10.1016/j.engstruct.2019.04.084
Nagarajaiah, S. and Erazo, K. (2016), "Structural monitoring and identification of civil infrastructure in the United States", *Struct. Monitor. Maint.*, *Int. J.*, **3**(1), 51-69. https://doi.org/10.12989/smm.2016.3.1.051
Naser, A.H., Badr, A.H., Henedy, S.N., Ostrowski, K.A. and Imran, H. (2022), "Application of Multivariate Adaptive Regression Splines (MARS) approach in prediction of compressive strength of eco-friendly concrete", *Case Studies Constr. Mater.*, **17**, e01262. https://doi.org/10.1016/j.cscm.2022.e01262
Panda, A.K. and Modak, S.V. (2022), "An FRF-based perturbation approach for stochastic updating of mass, stiffness and damping matrices", *Mech. Syst. Signal Process.*, **166**, p. 108416. https://doi.org/10.1016/j.ymssp.2021.108416
Park, H.S., Kim, J. and Oh, B.K. (2019), "Model updating method for damage detection of building structures under ambient excitation using modal participation ratio", *Measurement*, **133**, 251-261. http://doi.org/10.1016/j.measurement.2018.10.023
Qasem, S.N. and Shamsuddin, S.M. (2011), "Radial basis function network based on time variant multi-objective particle swarm optimization for medical diseases diagnosis", *Appl. Soft Comput.*, **11**(1), 1427-1438. http://doi.org/10.1016/j.asoc.2010.04.014
Qin, S.Q., Zhang, Y.Z., Zhou, Y.L. and Kang, J.T. (2018), "Dynamic model updating for bridge structures using the kriging model and PSO algorithm ensemble with higher vibration modes", *Sensors*, **18**(6), 1879. https://doi.org/10.3390/s18061879
Queipo, N.V. and Nava, E. (2019), "A gradient boosting approach with diversity promoting measures for the ensemble of surrogates in engineering", *Struct. Multidiscipl. Optimiz.*, **60**(4), 1289-1311. https://doi.org/10.1007/s00158-019-02325-4
Ren, W.X. and Chen, H.B. (2010), "Finite element model updating in structural dynamics by using the response surface method", *Eng. Struct.*, **32**(8), 2455-2465. https://doi.org/10.1016/j.engstruct.2010.04.019
Ren, X.Y., Wang, Y.M., Guo, T. and Wang, Q. (2020), "Robust Adaptive Beamforming Using Support Vector Machines", *IEEE Access*, **8**, 137955-137965. http://doi.org/10.1109/Access.2020.3009993
Roy, D.K. and Datta, B. (2019), "An ensemble meta-modelling approach using the Dempster-Shafer theory of evidence for developing saltwater intrusion management strategies in coastal aquifers", *Water Resour. Manag.*, **33**, 775-795. https://doi.org/10.1007/s11269-018-2142-y
Sarmadi, H., Entezami, A., Saeedi Razavi, B. and Yuen, K.V. (2021), "Ensemble learning-based structural health monitoring by Mahalanobis distance metrics", *Struct. Control Health Monitor.*, **28**(2), e2663. https://doi.org/10.1002/stc.2663
Sener, O. and Savarese, S. (2017), "Active learning for convolutional neural networks: A core-set approach", arXiv preprint arXiv:1708.00489. https://doi.org/10.48550/arXiv.1708.00489
Siddiqui, Y., Valentin, J. and Nießner, M. (2020), "Viewal: Active learning with viewpoint entropy for semantic segmentation", *Proceedings of the IEEE/CVF Conference on Computer Vision and Pattern Recognition*.
Sotoudehnia, E., Shahabian, F. and Sani, A.A. (2019), "An iterative method for damage identification of skeletal structures utilizing biconjugate gradient method and reduction of search space", *Smart Struct. Syst.*, *Int. J.*, **23**(1), 45-60. https://doi.org/10.12989/sss.2019.23.1.045
Sousa, H., Santos, L.O. and Chryssanthopoulos, M. (2019), "Quantifying monitoring requirements for predicting creep deformations through Bayesian updating methods", *Struct. Safety*, **76**, 40-50. http://doi.org/10.1016/j.strusafe.2018.06.002
Tran-Ngoc, H., Khatir, S., De Roeck, G., Bui-Tien, T., Nguyen-Ngoc, L. and Wahab, M.A. (2018), "Model updating for Nam O bridge using particle swarm optimization algorithm and genetic algorithm", *Sensors*, **18**(12), 4131. http://doi.org/ARTN 413110.3390/s18124131
Vapnik, V. (1999), *The Nature of Statistical Learning Theory*, Springer Science & Business Media.
Wang, Z. and Cha, Y.-J. (2021), "Unsupervised deep learning approach using a deep auto-encoder with a one-class support vector machine to detect damage", *Struct. Health Monitor.*, **20**(1), 406-425. https://doi.org/10.1177/1475921720934051
Wang, Z.Y. and Shafieezadeh, A. (2020), "Highly efficient Bayesian updating using metamodels: An adaptive Kriging-based approach", *Struct. Safety*, **84**, 101915. https://doi.org/10.1016/j.strusafe.2019.101915
Wang, Y.H., Lv, J., Feng, Y., Dai, B.W., Wang, C., Wu, J. and Chen, Z.Y. (2021), "Implementation of online model updating with ANN method in substructure pseudo-dynamic hybrid simulation", *Smart Struct. Syst.*, *Int. J.*, **28**(2), 261-273. https://doi.org/10.12989/sss.2021.28.2.261
Weng, S., Zhu, H., Xia, Y., Li, J. and Tian, W. (2020), "A review on dynamic substructuring methods for model updating and damage detection of large-scale structures", *Adv. Struct. Eng.*, **23**(3), 584-600. https://doi.org/10.1177/1369433219872429
Xing, Z.X., Qu, R.Z., Zhao, Y., Fu, Q., Ji, Y. and Lu, W.X. (2019), "Identifying the release history of a groundwater contaminant source based on an ensemble surrogate model", *J. Hydrol.*, **572**, 501-516. http://doi.org/10.1016/j.jhydrol.2019.03.020
Ye, P.C., Pan, G. and Dong, Z.M. (2018), "Ensemble of surrogate based global optimization methods using hierarchical design

space reduction", *Struct. Multidiscipl. Optimiz.*, **58**(2), 537-554. http://doi.org/10.1007/s00158-018-1906-6

Zhang, Y., Kim, C.W., Tee, K.F., Garg, A. and Garg, A. (2018), "Long-term health monitoring for deteriorated bridge structures based on Copula theory", *Smart Struct. Syst., Int. J.*, **21**(2), 171-185. http://doi.org/10.12989/sss.2018.21.2.171

Zhang, Y., Kim, C.W. and Lin, J.M. (2019), "Removing Environmental Influences in Health Monitoring for Steel Bridges Through Copula Approaches", *Int. J. Steel Struct.*, **19**(3), 888-895. http://doi.org/10.1007/s13296-018-0170-3

Zhang, Y., Wei, K., Shen, Z.H., Bai, X.W., Lu, X.Z. and Soares, C.G. (2020), "Economic impact of typhoon-induced wind disasters on port operations: A case study of ports in China", *Int. J. Disaster Risk Reduct.*, **50**. https://doi.org/10.1016/j.ijdrr.2020.101719

Zhu, Z., Au, S.K., Li, B. and Xie, Y.L. (2020), "Bayesian operational modal analysis with multiple setups and multiple (possibly close) modes", *Mech. Syst. Signal Process.*, **150**, 107261. https://doi.org/10.1016/j.ymssp.2020.107261

Zhu, H.P., Li, J.J., Tian, W., Weng, S., Peng, Y.C., Zhang, Z.X. and Chen, Z.D. (2021), "An enhanced substructure-based response sensitivity method for finite element model updating of large-scale structures", *Mech. Syst. Signal Process.*, **154**, 107359. https://doi.org/10.1016/j.ymssp.2020.107359

BS